Activation of the supraspinal opioid systems after peripheral noxious conditioning and inhibition of histone deacetylases

by

Kjærsti Johnsen

Master Thesis

Department of Molecular Biosciences, Faculty of Mathematics and Natural Sciences, University of Oslo, Norway

National Institute of Occupational Health, Oslo, Norway

January 2012

Takk!

Oslo, januar 2012

Arbeidet i denne masteroppgaven har blitt utført på Statens Arbeidsmiljøinstitutt, Oslo, og på Senter for molekylærbiologi og nevrovitenskap ved UiO.

Først vil jeg takke min hovedveileder Johannes Gjerstad for suveren veiledning og støtte gjennom disse to årene. Du skal også ha en stor takk for å ha tatt oss masterstudenter med på både store og små eventyr.

Hjertelig takk til deg også Linda Margareth Pedersen. Du er fantastisk! Jeg har vel brukt deg som Johannes sin høyre hånd igjennom denne tiden enten du ville det eller ikke. Unnskyld for det Linda, men du har tatt det med et smil. Tusen takk!

Jeg vil også rette en stor takk til alle involverte i PET studien, og da spesielt til Frode Willoch som gjorde det mulig for meg å inkludere PET i min oppgave, og til Trine Hjørnevik for å ha veiledet meg igjennom data analysen. Hong Qu fortjener også en varm takk. Takk for at du ofret din fritid for den praktiske gjennomføringen av PET studiet. Det hadde vært et umulig prosjekt uten deg.

I tillegg vil jeg takke resten av gjengen på STAMI, og da spesielt til Ada Ingvalsen, Line Melå Jacobsen og Audun Trygge Haugen Bersaas. Tusen takk for all hjelp på laben og mange gode tips på veien.

Også har vi de to søte tuppene som sitter i 1.etg, Maria Belland Olsen og Nina Gran Egeland. Tusen takk for gode råd og mange fine stunder. Dere er nydelige begge to, og jeg ønsker dere all lykke i fremtiden.

Sist men ikke minst, tusen, hjertelig takk til mine kjære foreldre som alltid er der for meg.

Kjærsti Johnsen

Abstract

Previous studies show that the endogenous opioid system has an important role in the pain control system. In recent years, it has also been suggested that epigenetic modifications, such as acetylations, may affect pain sensitivity. Inhibition of histone deacetylases (HDACs) might lead to analgesia through prolonged activation of the NF-κB pathway, followed by an upregulation of mGlu2/3 receptors. Activation of mGlu2/3 receptors on the primary afferent neurons is believed to have an antinociceptive effect through inhibition of spinal glutamate release, and consequently on the spinal and supraspinal nociceptive transmission.

To investigate the activation of the supraspinal opioid system to noxious peripheral stimuli, spinal long-term potentiation (LTP) was induced by high frequency stimulation (HFS) conditioning applied to the sciatic nerve. Opioid tracer binding, i.e. opioid receptor (OR) availability, was measured prior and subsequent to the HFS conditioning by positron emission tomography (PET) imaging with the OR agonist radioligand [^{18}F]PEO. To further investigate the potential effect of HDAC inhibition on the supraspinal opioid system, a group of animals were pretreated with the HDAC inhibitor MS-275 (3 mg/kg s.c.) once every 24 h for 5 consecutive days prior to the PET scans. RT-qPCR was applied to investigate changes in gene expression encoding the OR-μ, OR-κ, pre-proenkephalin and cholecystokinin B receptors in the ipsilateral hippocampus, due to their potential role regarding the opioidergic system.

The present study demonstrated that induction of spinal LTP by HFS conditioning was associated with a reduced opioid tracer binding in the ipsilateral primary somatosensory cortex, visual cortex, and hippocampus. The observed decrease in opioid tracer binding is most likely explained by an increase in the endogenous opioid peptide release. Similar observation was done in the somatosensory cortex of the MS-275 pretreated animals. However, the reduction in opioid tracer binding was less pronounced compared with the untreated animals. Notably, no significant changes in opioid tracer binding were observed in the other parts of the brain, i.e. visual cortex and hippocampus, in the pretreated animals. Hence, an overall tendency of reduced activation of the endogenous opioid

system was observed in the MS-275 pretreated animals compared with the untreated animals. The gene expression analyses did not show any significant changes in the expression of the target genes after HFS conditioning.

In conclusion, the present findings suggest that a peripheral noxious stimulation that induces spinal LTP may activate the supraspinal OR system, especially in the hippocampus. This activation seems to be less pronounced after inhibition of HDACs. This may imply that inhibition of HDACs attenuate the activation of the OR system upon induction of LTP.

Table of contents

Abbreviations

AMPA	α-amino-3hydroksy-5-methyl-4-isoxazolepropionic
ANCOVA	Analysis of covariance
ATP	Adenosine triphosphate
bp	Base pair
CA	Cornu ammonis
CaMKII	Calcium/calmodulin dependent kinase II
cAMP	3’-5’-cyclic adenosine monophosphate
CCK	Cholecystokinin
CCK_A	Cholecystokinin A
CCK_B	Cholecystokinin B
Cckbr	Cholecystokinin B receptor
cDNA	Complementary DNA
CNS	Central nervous system
C_q	Quantification cycle
CREB	3’-5’-cyclic adenosine monophosphate (cAMP) response-element binding protein
DMSO	Dimethyl sulfoxide
EPSP	Excitatory postsynaptic potential
ERK	Extracellular signal-regulated kinase
GABA	γ-aminobutyric acid
GC	Guanine/Cytosine
GIRK	G-protein-activated inwardly rectifying potassium channel
Glu	Glutamate
GPCR	G-protein coupled receptor
HAT	Histone acetyltransferase
HDAC	Histone deacetylase
HFS	High frequency stimulation
IP_3	Inositol 1,4,5-triphosphate
K^+	Potassium
LC	Locus coeruleus
LTP	Long-term potentiation
MBq	Megabecquerel
mGluR	Metabotropic glutamate receptor

MRI	Magnetic resonance imaging
MS-275	N-[[4-[[(2-aminophenyl)amino]carbonyl]phenyl]methyl]-3-pyridinylmethyl ester
NA	Nucleus accumbens
NF-κB	Nuclear factor κB
NK1	Neurokinin 1
NMDA	N-methyl-D-aspartate
OD	Optical densitometry
Oprd1	Opioid receptor delta 1
Oprk1	Opioid receptor kappa 1
Oprm1	Opioid receptor mu 1
OR	Opioid receptor
PAG	Periaqueductal grey
PDYN	Pre-prodynorphin
PENK	Pre-proenkephalin
PET	Positron emission tomography
PKA	Protein kinase A
PKC	Protein kinase C
PLC	Phospholipase C
POMC	Pre-proopiomelanocortin
RIN	RNA Integrity Number
RNA	Ribonucleic acid
rRNA	Ribosomal ribonucleic acid
RT-qPCR	Reverse transcription quantitative polymerase chain reaction
RVM	Rostral ventromedial medulla
s.c.	Subcutaneously
SD	Sprague Dawley
SEM	Standard error of the mean
SP	Substance P
SUV	Standardized uptake value
TE	Tris/EDTA
T_m	Melting temperature
UV	Ultraviolet
VOI	Volumes of interest
WDR	Wide dynamic range

1 Introduction

1.1 Pain versus nociception

Pain is defined as an unpleasant sensory and emotional experience associated with actual or potential tissue damage, or described in terms of such damage (Loeser and Treede 2008). According to this definition, pain is a complex experience that involves not only the transduction of noxious stimuli, but also cognitive and emotional processing in the brain. Nociception, however, is defined as the neural processes of encoding and processing noxious stimuli (Loeser and Treede 2008). While pain is a subjective phenomenon, nociception is the object of sensory physiology including activation of specialized receptors, i.e. nociceptors, and specialized pathways activated by stimulation of the nociceptors. Even though nociception may be the underlying cause of many painful states, pain may occur without nociception and vice versa.

1.2 The nociceptive signaling- and modulatory system

1.2.1 Primary afferent nerve fibers

The primary afferent nerve fibers respond to a variety of sensory modalities including mechanical, thermal, and chemical stimuli. There are four main classes of primary afferents in the peripheral nervous system: Aα-, Aβ-, Aδ-, and C-fibers. Each has distinct anatomical- and functional properties, which enables them to respond to and transmit different types of sensory information. Aα- and Aβ- fibers are thickly myelinated with large axon diameters, high speed of conduction, and low activation threshold. While the fastest Aα-fibers transmit sensory information related to proprioception, Aβ-fibers normally convey tactile information. The thinly myelinated Aδ-fibers and the unmyelinated C-fibers have medium and small axon diameters, respectively, and consequently slower speed of conduction. They possess high activation thresholds, and transmit noxious mechanical, thermal, or chemical stimuli. Therefore, the Aδ- and C-fibers are referred to as nociceptors. The nociceptors innervate most of the tissue in the body including, skin, muscles, joints, and viscera, for review see (Willis and Westlund 1997). In general, when the nociceptors are stimulated, the nociceptive information is conducted from the periphery, via the dorsal root ganglion (or trigeminal ganglion), and into the dorsal horn of the spinal cord.

1.2.2 The spinal dorsal horn and ascending pathways

The dorsal horn of the spinal cord is organized into six anatomical distinct laminae (I-VI). While most Aα- and Aβ-fibers project to the deeper laminae III-VI in the dorsal horn, the C-fibers predominately project more superficially to lamina I and II. By contrast, Aδ-fibers predominately innervate lamina I as well as the deeper lamina V (Light and Perl 1979; Sugiura et al. 1986), for review see (Todd 2002). Within these laminae, the primary afferents make synaptic connections with dorsal horn neurons. Based on the projection of the axons, the dorsal horn neurons are divided into three general classes: propriospinal neurons, interneurons, and projection neurons. Propriospinal neurons transfer information from one segment of the spinal cord to another, and play a major role in controlling locomotion as well as reflex responses. The vast majority of intrinsic dorsal horn neurons are interneurons. They are localized within one segment, and synapse both presynaptically on primary afferent nerve endings and postsynaptically on dorsal horn neurons. They comprise both excitatory- (glutamatergic) and inhibitory (GABAergic and glycinergic) interneurons, and are believed to have a modulatory function on neural processing, including nociception. Projection neurons transfer sensory information from the spinal cord via the parabrachial area to supraspinal centers, including amygdala, hypothalamus, thalamus, and somatosensory cortex (Burstein et al. 1987; Hylden et al. 1989; Wiberg et al. 1987). These centers, contribute to the affective component of the pain experience. Information about the location and intensity of a noxious stimulus is predominately conveyed by projection neurons from the spinal cord to the somatosensory cortex via the thalamus. Based on their synaptic input, the projection neurons are divided into distinct classes. Cells that receive input exclusively from Aβ-fibers are low threshold mechanosensitive cells, and respond to innocuous stimuli. Nociceptive specific (NS) cells receive information from Aδ- and C-fibers only, and are activated exclusively by noxious stimuli. In contrast, wide dynamic range (WDR) cells receive input from Aβ-, Aδ- and, C-fibers, hence responding to the full range of mechanical, thermal, and chemical stimuli, for review see (D'Mello and Dickenson 2008).

1.2.3 Descending modulatory system

A complex descending modulatory system may control the activity in the ascending pathways. This modulatory system originates mainly in prefrontal cortex, anterior cingulate cortex, insular cortex, hypothalamus, and amygdala (Beitz 1982; Hardy and Leichnetz 1981; Hopkins and Holstege 1978). From the supraspinal centers, and from sites in the brainstem, there are direct projections to the periaqueductal grey (PAG) (Beitz 1982), which integrates supraspinal information with ascending nociceptive input from the dorsal horn. The nociceptive modulating action of the PAG on the spinal cord is predominately relayed through the rostral ventromedial medulla (RVM). There are three distinct populations of neurons in the RVM: On-cells, Off-cells, and neutral cells (Fields and Heinricher 1985). The efficacy of nociceptive transmission in the dorsal horn of the spinal cord is largely influenced by the On- and Off-cells, which may have a facilitatory effect (On-cells) or an inhibitory effect (Off-cells) on nociception (Bederson et al. 1990; Foo and Mason 2003; Heinricher et al. 1989). Moreover, the nociceptive transmission in the spinal cord is also modulated by projections from the locus coeruleus (LC) (Jones and Gebhart 1986). Thus, the nociceptive modulatory system is a complex network, which integrates information from different areas in the brain, the brainstem, and the spinal dorsal horn (Figure 1).

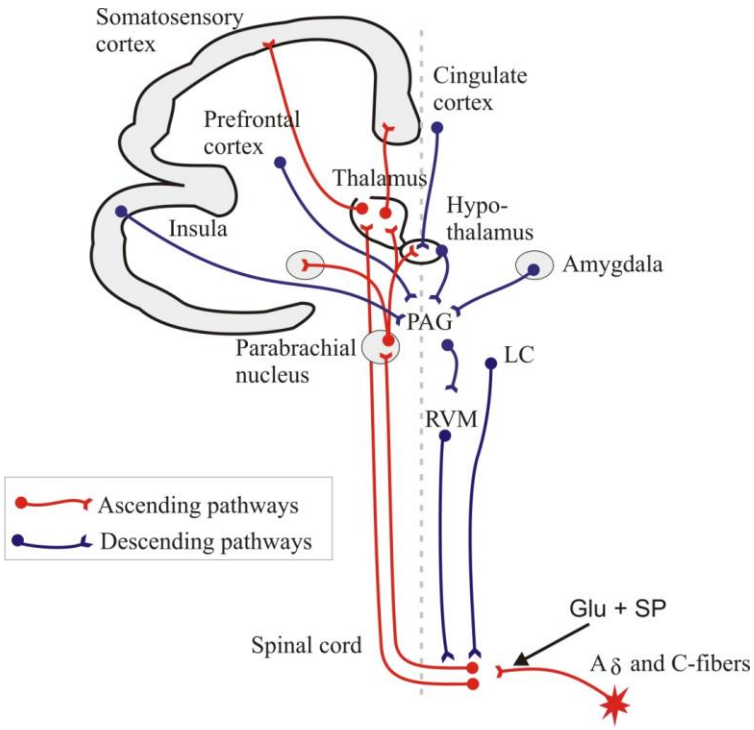

Figure 1. A simplified presentation of the nociceptive signaling- and modulatory pathways. Aδ- and C-fibers convey nociceptive information via projection neurons within the dorsal horn of the spinal cord to the brainstem and supraspinal centers, including parabrachial nucleus, thalamus, hypothalamus, amygdala, and somatosensory cortex. Complex descending pain-modulatory pathways from supraspinal sites such as prefrontal cortex, cingulate cortex, insula, hypothalamus, and amygdala, to the PAG, which via RVM project to the spinal dorsal horn and modulate the spinal activity, and thereby the ascending pathways. The spinal activity is also modulated by additional projections from the LC to the spinal cord. Glu: glutamate, LC: locus coreuleus, PAG: periaqueductal grey, RVM: rostral ventromedial medulla, SP: substance P. Adapted from (Gjerstad 2007).

1.3 Synaptic plasticity in the central nervous system (CNS)

Tissue and nerve injuries may produce plastic changes in the central pain pathways with enhanced nociceptive transmission from the spinal cord to the brain as one possible consequence. This phenomenon is called central sensitization, and is defined as an increased responsiveness of nociceptive neurons in the CNS to their normal afferent input (Loeser and Treede 2008). Central sensitization is believed to be critical for the development of different pain states where hypersensitivity in the CNS is likely to occur, and may involve multiple cellular processes, including increased membrane excitability, enhanced synaptic efficacy, and/or decreased inhibitory transmission (disinhibition), for reviews see (Latremoliere and Woolf 2009; Woolf and Salter 2000). There are many similarities between central sensitization and long-term potentiation (LTP), and it has been suggested that LTP is a form of central sensitization or possibly vice versa, for review see (Willis 2002). The first experimental data of the existence of LTP came in the 1970s, when Bliss and Lømo demonstrated that intense high-frequency trains of electrical stimulations of hippocampal neurons, resulted in long-lasting changes in the synaptic efficacy (Bliss and Lomo 1973). Similar synaptic changes have later been demonstrated in other parts of the CNS including the spinal cord (Liu and Sandkuhler 1995; Randic et al. 1993; Rogan et al. 1997).

1.3.1 Cellular mechanisms of spinal LTP

Brief low intensity stimulation of the primary afferent A-fibers is normally transduced by glutamate (Glu) release and subsequent activation of the ionotropic α-amino-3hydroksy-5-methyl-4-isoxazolepropionic (AMPA) receptors on the post-synaptic membrane. Activation of these receptors leads to an influx of cations, which in turn generate fast excitatory postsynaptic potentials (EPSPs). However, if the stimulus intensity is high, increased co-release of Glu and substans P (SP) from the central terminals of the C-fibers may occur. Postsynaptic AMPA-, neurokinin 1 (NK1)- and metabotropic glutamate 1 (mGlu1) receptors are activated, which in turn may lead to a long-lasting postsynaptic depolarization, and subsequent activation of both voltage-gated calcium channels and ionotropic N-methyl-D-aspartate (NMDA) receptors. The NMDA receptors are, at resting membrane potential, inhibited by a voltage-dependent Mg^{2+} block and require both Glu and adequate depolarization for activation. Activation of both the voltage-gated calcium channels and the NMDA receptors leads to opening of the channels and a substantial Ca^{2+} influx. Additional Ca^{2+} is released from intracellular stores by activation of the phospholipase C (PLC)-inositol 1,4,5-triphosphate (IP_3) pathway through stimulation of the mGlu1- and the NK1 receptors.

The substantial increase in intracellular Ca^{2+} concentration is believed to be crucial for the onset of spinal LTP, and may result in activation of a variety of Ca^{2+}-dependent intracellular responses, including activation of protein kinase A (PKA), calcium/calmodulin dependent kinase II (CaMKII), the extracellular signal-regulated kinase (ERK), and additional activation of PKC (Lin et al. 1996; Lin et al. 2002; Rosen et al. 1994; Yang et al. 2004), for review see (Sandkuhler 2009). Activation of several of these protein kinases and subsequent signaling cascades, may induce phosphorylation of AMPA- and NMDA receptors. These receptor modifications may in turn enhance the channel opening time and recruitment of additional AMPA receptors to the postsynaptic membrane, thereby increasing the synaptic efficacy. In addition, there is evidence suggesting that PKC activation may promote sustained suppression of the Mg^{2+} blockade of the NMDA receptor (Chen and Huang 1992).

Although ERK is involved in cytosolic cellular signaling, it can also translocate to the nucleus where it phosphorylates and activates the transcription factor 3'-5'-cyclic adenosine monophosphate (cAMP) response-element binding protein (CREB). CREB may in turn bind to different promotor regions, thereby activating the transcription of a number of genes (Ji et al. 1999; Sgambato et al. 1998; Vanhoutte et al. 1999). Thus, ERK may be involved in both short-term and long-term effects on the neuronal excitability.

Recently, recruitment of glial cells have shown to play a major role in synaptic plasticity (Ma and Zhao 2002). Upon a noxious stimulus, activation of spinal neurons may result in release of neuromodulators such as adenosine triphosphate (ATP) and SP, which in turn can recruit and activate microglia. Activated microglia synthesize and release multiple neuroactive substances, including pro-inflammatory cytokines, which may increase the excitability of spinal neurons by enhancing the transmitter release or the function of the NMDA- and AMPA receptors. Cytokines may also further activate other surrounding glial cells, for reviews see (McMahon et al. 2005; Milligan and Watkins 2009).

1.4 The endogenous opioid system

Opium derivatives such as morphine have for centuries been known to have an analgesic effect. In the early 1970s, the existence of high affinity stereospecific receptors for different opiate drugs were demonstrated in the brain (Martin et al. 1976; Pert and Snyder 1973; Terenius 1973) followed by pharmacological studies purposing three different opioid receptor types. These are referred to as mu (μ), delta (δ), and kappa (κ) opioid receptors (Martin et al. 1976) and are encoded by the three genes *Oprm1*, *Oprd1*, and

Oprk1, respectively. The receptors have high structural homology with the best conserved domains within the seven-transmembrane helical core containing the opioid-binding pocket, for reviews see (Kieffer 1995; Kieffer and Evans 2009). The endogenous ligands of the opioid receptors (ORs) are identified as a family of more than 20 known opioid peptides. These are grouped into three main classes: the endorphins, the enkephalins, and the dynorphins. Each of these classes are liberated from an inactive pre-propeptide: pre-proopiomelanocortin (POMC), pre-proenkephalin (PENK), and pre-prodynorphin (PDYN), respectively. Evidence exists that POMC derivatives, such as β-endorphins, may bind equally to μ- and δ receptors, whereas enkephalins and dynorphins have greatest affinity to δ- and κ receptors, respectively (Chavkin et al. 1982).

The opioid receptors belong to the seven-transmembrane G-protein coupled receptor (GPCR) family, and interact with G_0/G_i inhibitory proteins. When the receptors are stimulated, the G-protein subunits dissociate from the receptors, and may activate multiple intracellular second messenger systems. Several opioid-evoked signaling events have been identified. These may include reduced neuronal excitability by inhibition of voltage-dependent Ca^{2+} channels, and stimulation of G-protein-activated inwardly rectifying potassium channels (GIRKs) (Ikeda et al. 2002). Depending on whether the receptors are located pre- or postsynaptic, activation leads to inhibition of neurons by decreasing either neurotransmitter release or neuronal excitability by opening of K^+ channels. It has also been demonstrated that opioids may stimulate PLC and inhibit adenylyl cyclase activity, both affecting cytoplasmic events and the transcriptional activity of the cell, for reviews see (Kieffer and Evans 2009; Williams et al. 2001). The receptors are expressed on both excitatory and inhibitory neurons, and the consequence of receptor activation within the neural circuits can therefore be inhibition or disinhibition. Furthermore, it is believed that the endogenous opioid peptides may contribute to antinociception by activating the PAG-RVM system, and thereby initiating the descending inhibition of nociceptive processing.

However, in recent years several lines of evidence have demonstrated that dynorphin may participate in pronociceptive processes. Although these mechanisms are not fully understood, it has been proposed that spinal dynorphins may promote excitatory transmitter release from the primary afferent terminals through interaction with the

NMDA receptors and/or bradykinin receptors (Lai et al. 2006; Laughlin et al. 1997; Rady et al. 1999). Supraspinally, their pronociceptive actions seem to occur in an OR dependent manner through direct inhibition of RVM Off-cells, and thereby attenuating μ-opioid induced analgesia (Bie and Pan 2003; Meng et al. 2005; Pan et al. 1997), for reviews see (Laughlin et al. 2001; Millan 2002; Pan 1998).

The ORs and their ligands exist throughout the peripheral- and central nervous system including hippocampus, insular cortex, amygdala, PAG, RVM, hypothalamus, and the spinal cord (Gray et al. 2006; Mansour et al. 1995). Several studies have suggested that the endogenous opioid system regulates nociception, hedonic homeostasis, and stress responses, and in addition is involved in many other physiological responses (Kieffer and Gaveriaux-Ruff 2002).

1.4.1 Endogenous opioid peptides and cholecystokinin (CCK)

Cholecystokinin (CCK) is a brain-gut peptide, acting through its receptors both in the periphery, and in the CNS. Two subtypes of CCK receptors have been identified: cholecystokinin A receptors (CCK_A), the most prominent receptor subtype peripherally, and cholecystokinin B receptors (CCK_B), which are mainly expressed in the CNS, including amygdala, ventral tegmental area, thalamus, hypothalamus, nucleus accumbens, hippocampus, PAG, and the spinal cord (Kritzer et al. 1988; Mercer et al. 2000; Moran et al. 1986; Noble and Roques 1999). There are several lines of evidence suggesting that CCKs act as functional antagonists to the analgesic action of opioids (Crawley and Corwin 1994; Faris et al. 1983; Li and Han 1989; Watkins et al. 1985; Wiesenfeld-Hallin et al. 2002). Although the mechanisms by which CCK antagonizes opioid induced analgesia is not fully understood, it has been suggested that CCK, via activation of the CCK receptors, may modify the ORs and consequently the binding affinity for their endogenous opioid ligands (Wang et al. 1989; Wang and Han 1990). It has also been suggested that CCK may inhibit the synthesis or the release of enkephalins (Ossipov et al. 1994). Furthermore, there are data suggesting that CCK might activate On-cells in the RVM, and thereby facilitate the descending pronociceptive signaling (Heinricher and Neubert 2004; Kovelowski et al. 2000). Finally, CCK has also been shown to prevent the opioid induced activation of Off-cells (Heinricher et al. 2001), for review see (Lovick

2008). Thus, CCK may attenuate the antinociceptive action of opioids by acting both spinally and supraspinally.

1.5 Epigenetic regulation

Induction and maintenance of persistent pain involves long-term molecular changes. These changes are usually caused by altered gene expression and subsequent protein synthesis. It has been suggested that epigenetic mechanisms such as DNA methylation and histone acetylation may influence the transcription of various genes, including genes involved in pro- and antinociceptive processes.

DNA is packed into a highly organized structure called 30 nm chromatin fiber, which in addition to DNA also consists of histone and non-histone proteins. The basic units of chromatin are the nucleosomes, which are separated from each other by linker DNA resulting in a beads-on-a-string arrangement. Each nucleosome consists of DNA wound twice around an octamer composed of two molecules each of the four main histone types: H2A, H2B, H3, and H4 (Peterson and Laniel 2004). The amino acid side chains of the histone proteins can undergo various types of modification, including covalent modifications such as acetylation, methylation, phosphorylation, and ubiquitylation. Especially the N-terminal histone tails, which extend from the nucleosome octamer, are exposed. These reversible post-translational modifications are believed to be involved in processes such as gene transcription, DNA repair, and apoptosis.

1.5.1 Acetylation

Histone acetylation is thought to have a prominent role in the regulation of genome expression, and is controlled by two counteracting enzymes: histone acetyltransferases (HATs) and histone deacetylases (HDACs). Whereas HATs catalyze the addition of acetyl groups and are associated with enhanced gene transcription, HDACs remove acetyl groups from the histones, and promote gene silencing. Histone acetylation is believed to destabilize the 30 nm chromatin fiber, thereby exposing the DNA to the transcriptional machinery (Norton et al. 1989; Vettese-Dadey et al. 1996). Furthermore, acetylation may facilitate, and regulate transcriptional processes by providing docking sites for different proteins, including additional histone modifying enzymes, as well as transcription factors (Felsenfeld and Groudine 2003), for review see (Barrett and Wood 2008). In addition to histones, a number of non-histone proteins are also subject to regulation by acetylation. These include transcription factors such as nuclear factor κB (NF-κB) (Ashburner et al. 2001; Glozak et al. 2005; Spange et al. 2009). Recent studies have suggested that acetylation by HATs and deacetylation by HDACs may have an influence on different pain states through the activation or inhibition of the NF-κB pathway, respectively (Chiechio et al. 2009b). Acetylation of NF-κB promotes transcription of NF-κB regulated genes, including genes encoding metabotropic glutamate 2 and 3 (mGlu2/3) receptors (Chiechio et al. 2009a). mGlu2/3 receptors are expressed throughout the nervous system, including on the peripheral terminals of primary afferent neurons, and on presynaptic terminals in the dorsal horn of the spinal cord (Azkue et al. 2000; Carlton et al. 2001; Jia et al. 1999). These receptors interact with G_0/G_i inhibitory proteins, and it is suggested that activation may depress the nociceptive transmission through inhibition of adenylyl cyclase, inhibition of voltage-sensitive Ca^{2+} channels, and/or activation of GIRKs (Dutar et al. 1999; Gerber and Gahwiler 1994; Knoflach and Kemp 1998; Mills et al. 2002; Sharpe et al. 2002; Simmons et al. 2002; Yang and Gereau 2002), for reviews see (Carlton et al. 2009; Niswender and Conn 2010). Hence, it is proposed that HATs, or alternatively inhibition of HDACs, may lead to analgesia through activation of the NF-κB pathway and subsequent upregulation of mGlu2/3 receptors (Chiechio et al. 2009b).

2 Aims

The main purpose of this study was to investigate how peripheral noxious conditioning, which induce spinal LTP, may affect the supraspinal endogenous opioid system, and whether these changes may be epigenetic modulated by inhibition of histone deacetylases (HDACs). More specifically the study aimed to:

I) Explore how induction of spinal LTP by HFS conditioning applied to the sciatic nerve affects the endogenous opioid system in the rat brain.

II) Investigate whether the HDAC inhibitor MS-275 affects the endogenous opioid system at rest and after induction of spinal LTP by HFS conditioning.

III) Examine if induction of spinal LTP by HFS conditioning is associated with altered hippocampal expression of the genes encoding the opioid receptors μ, δ and κ, in addition to pre-proenkephalin and cholecystokinin B receptors.

3 Materials and Methods

All animal experiments were approved by the Norwegian Animal Research Authority (NARA), and were performed in conformity with the laws and regulations controlling experiments and procedures on live animals in Norway. These laws are in accordance with the European convention for the protection of vertebrate animals used in experimental and other scientific purposes.

3.1 Animals

Adult female Sprague Dawley (SD) rats (Scanbur, Sweden) weighing 200-250 g, were used in all experiments. Different animals were used in the PET study and the gene expression study. The rats were housed in the animal facility at Oslo University Hospital Rikshospitalet and the National Institute of Occupational Health, where the air temperature was kept at 20-25 °C with a relative humidity at 50-55%. The rats had free access to food and water, and were acclimatized at least one week before the experiments were performed. All experiments were performed during the light period of a 12h/12h light/dark cycle. The rats were sacrificed immediately after the experiments.

3.2 Surgery

The experiments were performed under gas anaesthesia with isoflurane (Abbott Laboratories, Illinois, USA): 5 % for induction, and 2 % for maintenance. Surgical level of anaesthesia was verified by the absence of hind paw withdrawal to pinch. At the mid-thigh level, a section of 8-10 mm of the left sciatic nerve was dissected free and isolated from surrounding tissue by a plastic film. A bipolar silver hook electrode was placed proximal to the main branches of the sciatic nerve for high frequency stimulation (HFS) conditioning, i.e. 1 ms rectangular pulses, 4.5 mA, five trains of 1 s duration, 100 Hz, 10 s intervals between the trains. The rat´s core temperature was kept constant at 36-37 °C by means of an electrical feedback heating pad (Harvard homeothermic blanket control unit, Harvard Apparatus LTD, Kent, UK), and Simplex, i.e. 80 % vaseline and 20 % paraffin, was used to prevent dry eyes.

3.3 Positron emission tomography (PET) study

3.3.1 Drug administration

The class I histone deacetylase (HDAC) inhibitor N-[[4-[[(2-aminophenyl)amino]carbonyl]phenyl]methyl]-3-pyridinylmethyl ester (MS-275) (AH diagnostics as; Cayman Chemical Company) was used in the PET study. Following the supplier's protocol, MS-275 was dissolved in 100 % dimethyl sulfoxide (DMSO), stored at -20 °C, and diluted in 0.9 % NaCl the same day as administered. A dose of 3 mg/kg body weight MS-275 dissolved in 5 % DMSO was injected subcutaneously (s.c.) once every 24 h for 5 consecutive days, with the last injection the same day as the intervention (HFS) scan.

3.3.2 PET data acquisition and image analysis

PET data were acquired at the Small Animal Imaging Unit of the Center for Molecular Biology and Neuroscience, University of Oslo, Norway, by use of a high sensitivity (6.5%) small animal PET scanner (microPET Focus 120, Siemens Medical Solutions, Erlangen, Germany) with high spatial resolution (< 1.45 mm FWHM, 2D FBP) (Kim et al. 2007).

The animals were divided into two groups; HFS ($n = 7$) and HFS_{MS-275} ($n = 7$). Both groups received HFS conditioning. In addition, the HFS_{MS-275} group was pretreated with MS-275 as described above. The opioid receptor (OR) agonist ligand [^{18}F]PEO (26 ± 8 MBq) (Department of Chemistry, University of Oslo, Norway) (Schoultz et al. 2012) was intravenously injected in the tail vein 30 min prior to all scans. Two 30 min scans were performed on each animal, i.e. baseline scan and HFS scan. Baseline scans were acquired for all animals the day prior to the HFS scan. The HFS scans were performed 180-210 min after HFS conditioning ([^{18}F]PEO injection 150 min after HFS conditioning) (Figure 2).

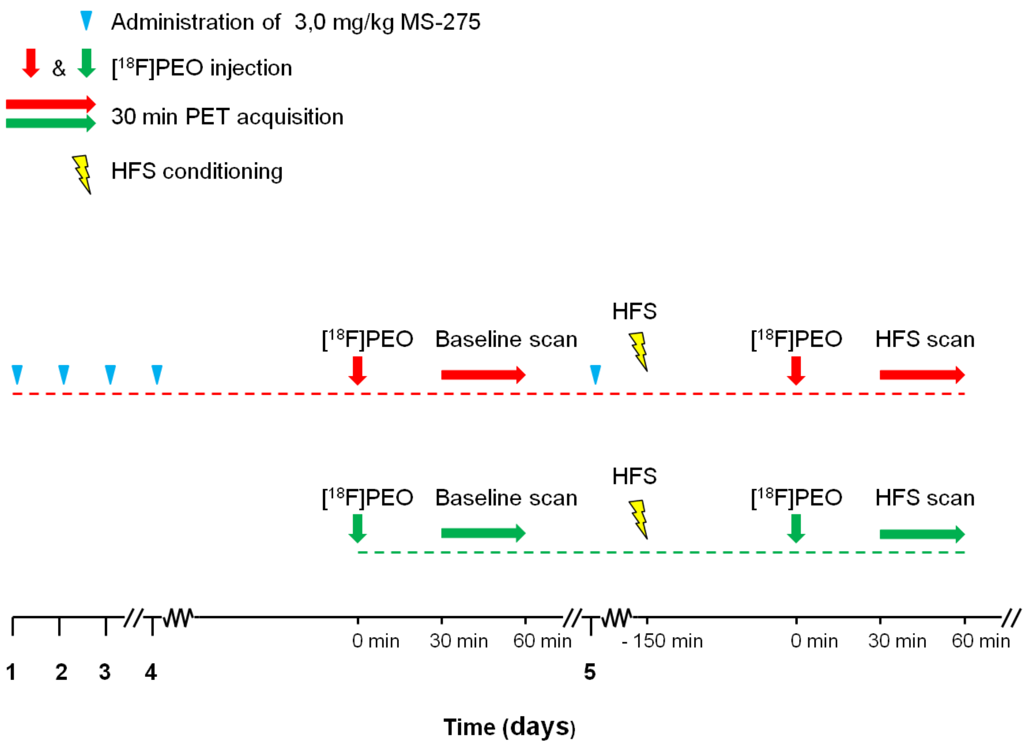

Figure 2. PET scan protocol. The animals were divided into two groups; HFS (green, *n* = 7) and HFS_{MS-275} (red, *n* = 7). HFS_{MS-275} group was pretreated with MS-275 subcutaneously once every 24 h for 5 consecutive days, with the last injection the same day as the HFS scan. Two 30 min scans were performed on each animal; baseline (at rest) and HFS (180-210 min after HFS conditioning). Baseline scans were acquired for all animals the day prior to the HFS scan. The OR agonist ligand [^{18}F]PEO (26 ± 8 MBq) was injected 30 min prior to all scans. HFS: high frequency stimulation, MBq: megabecquerel, OR: opioid receptor, PET: Positron emission tomography.

Data were collected in list mode using OSEM3D/MAP (Qi and Leahy 2000; Qi et al. 1998); 2 OSEM iterations, 18 MAP iterations, $\beta = 0.1$, $128 \times 128 \times 95$ matrix size, $0.87 \times 0.87 \times 0.80$ mm^3 voxel size. With regard to injected activity and body weight, all images were converted into normalized standardized uptake value (SUV) images in PMOD (PMOD Technologies Ltd., Zurich, Switzerland). Statistical analyses were performed with SPM8 (Wellcome Department of Cognitive Neurology, Institute of Neurology, London). Employing a 12-parameter affine transformation procedure, an intra-subject co-registration of the SUV images (HFS and baseline), and spatial normalization to a customized PET template was performed. The customized PET template was created from an average of the images of all animals. Furthermore, the images were smoothed with a 2 mm FWHM Gaussian filter to increase signal-to-noise ratio.

3.3.3 Data analysis and statistics

Statistical group analyses were performed on normalized (AnCova) images. Both, paired Student´s *t*-tests (HFS vs. baseline, and HFS_{MS-275} vs. baseline $_{MS-275}$), as well as two sample Student´s *t*-tests (baseline vs. $baseline_{MS-275}$, and HFS relative to baseline vs. HFS_{MS-275} relative to baseline $_{MS-275}$) were performed (Figure 3). Significance was accepted at the 1% level, and inference was tested for both increased and decreased PET signals.

For definition of anatomical structures, the significant image ($p \leq 0.01$), i.e. the parametric T-map obtained from the group analysis, was co-registered with an in-house magnetic resonance imaging (MRI) template fitted to the atlas “The Rat Brain in Stereotaxic Coordinates-2005” by Paxinos and Watson (Schweinhardt et al. 2003). In addition, for localization of the significant PET signals, the parametric T-map and the MRI template was co-registered with a 3-D digital atlas reconstructed from the same atlas as the MRI template (Hjornevik et al. 2007) (Figure 4). Statistical T-values in different brain regions were extracted and reported.

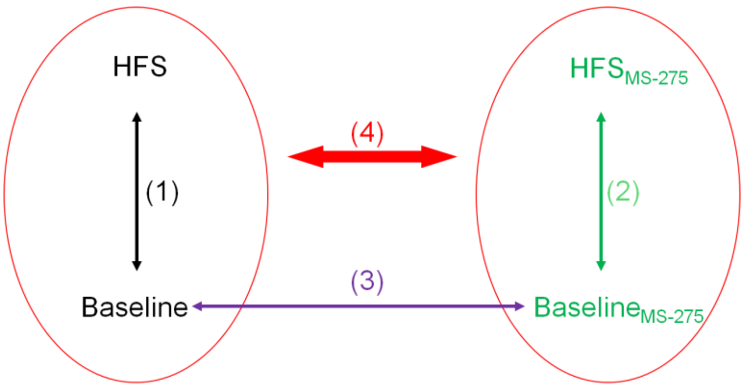

Figure 3. Statistical group analyses performed on PET data. Paired Student´s *t*-test: (1) HFS vs. Baseline, and (2) HFS_{MS-275} vs. baseline $_{MS-275}$. Two sample Student´s *t*-test: (3) baseline vs. $baseline_{MS-275}$, and (4) HFS relative to baseline vs. HFS_{MS-275} relative to baseline $_{MS-275}$. Significance was accepted at the 1% level, and inference was tested for both increased and decreased PET signals. HFS: high frequency stimulation, PET: Positron emission tomography.

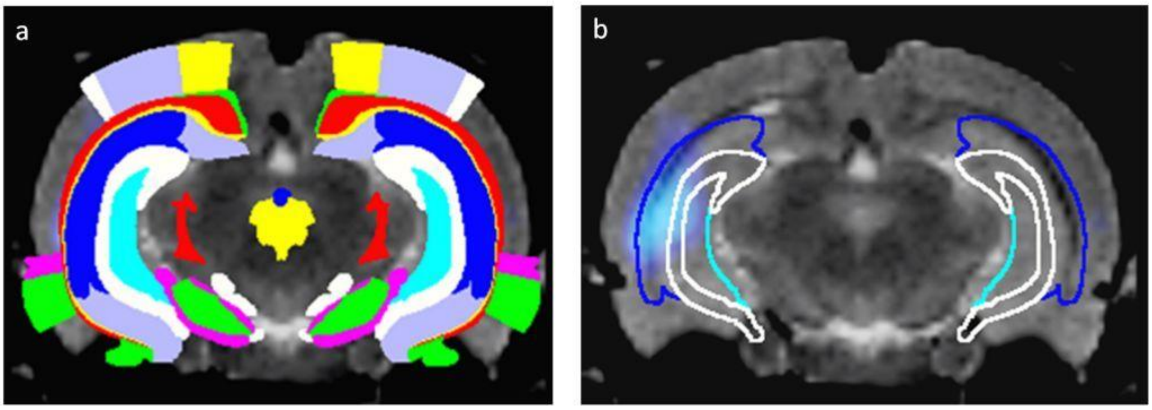

Figure 4. Example of how significant signals were localized by aid of a 3-D digital atlas reconstructed from "The Rat Brain in Stereotaxic Coordinates" by Paxinos and Watson (Hjornevik et al. 2007). Coronal representations of the rat brain. **(a)** A statistical significant PET image ($p \leq 0.01$) obtained from group analyses co-registered with a MRI template and a 3-D digital atlas. **(b)** Example of how regions with statistical T-values were identified by aid of a 3-D digital atlas (blue line: CA1, turquoise line: CA2&3, white line: dentate gyrus). CA: cornu ammonis, HFS: high frequency stimulation, MRI: magnetic resonance imaging, PET: Positron emission tomography.

3.4 Gene expression study

3.4.1 Tissue harvesting

Three different groups were included in the gene expression analyses: native group, control group, and HFS group. In the first group, tissue was harvested from native animals, i.e. immediately after anaesthesia and without surgery. In both the control and HFS group, the left sciatic nerve was isolated, and a hook electrode was placed around the nerve for 1 min. The HFS conditioning was applied only to the animals in the HFS group. At 180 min after the hook electrode was placed around the nerve, the animals were sacrificed. The brain was rapidly dissected out, divided in two, and within 5-6 min, frozen in liquid nitrogen. Tissue from hippocampus was isolated and stored at -80^{o}C for further analysis (Figure 5).

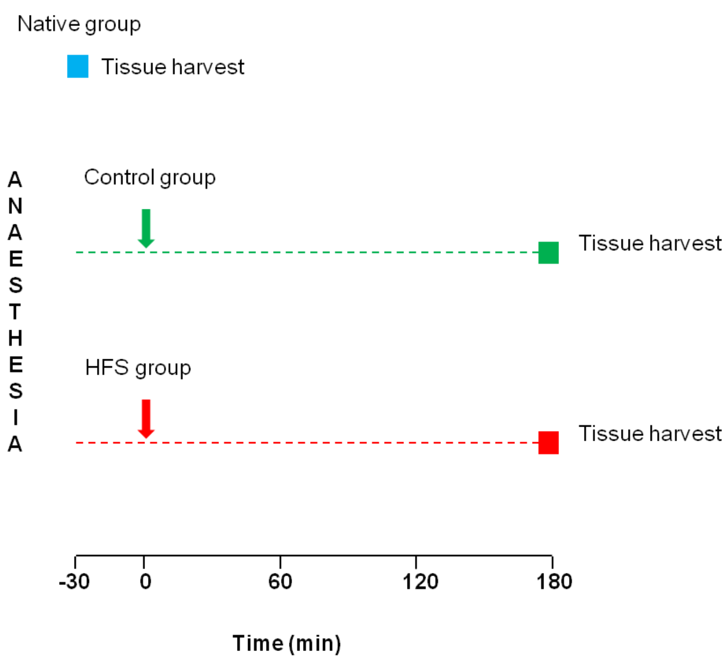

Figure 5. Protocol for tissue harvesting. The animals were divided into three groups indicated by the different colors: native group, control group, and high frequency stimulation (HFS) group. For both control and HFS group, the left sciatic nerve was isolated, and a hook electrode was placed around the nerve (indicated by the arrows). The tissue was harvested at the time indicated by the squares; immediately after anaesthesia for the native animals, and at time 180 min for the animals in the HFS or control group. Notably, only the animals in the HFS group received HFS conditioning.

3.4.2 RNA isolation from hippocampus tissue

For RNA isolation, tissue samples from the caudal part of the ipsilateral hippocampus were homogenized in TRIzol (Life technologies, Inc., Rockville, Maryland, USA) by a mixer mill (Retsch MM301, Haan, Germany). Non-soluble cell debris was removed by centrifugation. Chloroform was added to separate the sample into three phases: a lower organic phase, an interphase, and an upper aqueous phase. The aqueous phase with the RNA was extracted, and isopropanol was added for RNA precipitation. The pellet was washed with 75 % ethanol, dried, and re-dissolved in DEPC-water. To standardize the concentration in each sample, the amount of RNA was quantified by optical densitometry (OD), and then diluted in DEPC-water to a final concentration of 0.5 µg/µl (for further details see appendix I).

3.4.3 Evaluation of RNA quality

Agilent 2100 Bioanalyzer (Agilent Technologies, Waldbronn, Germany) was used for RNA quality control. To increase the efficacy of the lab procedure, total RNA from three groups were mixed together, denaturated at 70 °C, and applied into different wells on a microchip pretreated with gel matrix and a fluorescent dye. All RNA samples were run with RNA 6000 Nano Kit (Agilent Technologies, Waldbronn, Germany).

Each RNA sample was injected into a separation channel where the ribosomal subunits were electrophoretically separated. When bound to RNA, the fluorescence dye emits fluorescence, which is detected by laser induced fluorescence detection and translated into gel-like images and electropherograms. Based on this information, the software defined a RNA Integrity Number (RIN) value that was used to indicate the RNA quality (for further details see appendix II).

3.4.4 Complementary DNA (cDNA) synthesis

cDNA was synthesized from total RNA by the aid of first strand cDNA synthesis kit for reverse transcription quantitative polymerase chain reaction (RT-qPCR) (Roche Diagnostics, Mannheim, Germany). A mix of total RNA, deoxynucleotides, and random sequence primers were incubated at 65°C for 15 min. AMW reverse transcriptase and a reaction buffer were added, and the reverse transcription was performed at the following schedule: 42 °C for 60 min, 99 °C for 5 min, and 4 °C for 5 min (Perkin-Elmer Cetus DNA Thermal Cycler 480). The cDNA product was diluted in TRIS/EDTA (TE)-buffer to a final concentration of 10 ng/µl, and stored at -80 °C (for further details see appendix III).

3.4.5 Quantitative polymerase chain reaction (qPCR)

Gene expression analysis was performed on four different genes encoding the opioid receptor kappa 1 (*Oprk1),* opioid receptor mu 1 *(Oprm1),* cholecystokinin B receptor (*Cckbr),* and pre-proenkephalin *(Penk).* The analyses were performed on ABI 7900 (Applied Biosystems, Foster City, California, USA) with Perfecta SYBR Green Fastmix (Quanta Bioscience, Gaithersburg, MD, USA) at the following schedule: 90°C for 2 min, followed by 40 cycles of 95°C for 10 sec, and 60°C for 30 sec (for further details see appendix IV). *β-actin* was used as reference gene for normalization of gene expression.

The amount of template used in the qPCR reaction was cDNA corresponding to 50 ng reverse transcribed total RNA for *Oprk1*, *Oprm1*, *Cckbr*, *and Penk*, and 5 ng for *β-actin*. All primers (Table 1) were designed using the Primer Express 2.0 Software (Applied Biosystems, Foster City, California, USA) and checked for specificity by BLAST search (http://blast.ncbi.nlm.nih.gov/). To avoid amplification of possible DNA contamination, the forward- and reverse primers were separated by at least one intron on the corresponding genomic DNA.

Table 1. Primers used in quantitative polymerase chain reaction (qPCR).

Primer	Sequence (written 5´→ 3´)	bp	% GC	T_m°C	Product size (bp)
β-actin forward	CTA AGG CCA ACC GTG AAA AGA	21	47.6	58.0	87
β-actin reverse	ACA ACA CAG CCT GGA TGG CTA	21	52.4	59.2	
Penk forward	CTA AAT GCA GCT ACC GCC TG	20	55.0	57.3	191
Penk reverse	GTG GCT CTC ATC CTG TTT GCT	21	52.4	58.0	
Oprk1forward	GTG GGC TTA GTG GGC AAT TC	20	55.0	58.1	76
Oprk1 reverse	AGA TGT TGG TTG CGG TCT TCA	21	47.6	59.2	
Oprm1forward	CGT CTG CAA CTG GAT CCT CTC T	22	54.5	59.5	101
Oprm1 reverse	AGA ACG TGA GGG TGC AAT CTA TG	23	47.8	59.1	
Cckbr forward	GCT GTG ACC CCC CTC GTA T	19	63.2	58.4	101
Cckbr reverse	TCC GCC AAC ACT CAT CAG AA	20	50.0	58.8	

Each sample was screened for co-amplified products by generating a final melt curve of fluorescence versus temperature (Figure 6a). An amplification plot presented as delta Rn, i.e. a measure of emitted fluorescence intensity by the SYBR green bound PCR product as a function of number of cycles in the reaction, was also generated (Figure 6b). The quantification cycle (C_q) value, i.e. the number of cycles required for fluorescence signal to reach a computer defined threshold, was for each sample estimated with the software SDS 2.2 (Applied Biosystems, Foster City, California, USA). A dilution series (Figure 6c, d) was made to generate a standard curve (6e). The C_q value and the standard curve were then used to estimate the amount of target cDNA in each sample. The C_q value for a given sample corresponds to a specific amount of cDNA (Figure 6e). Non-template control was included in every run.

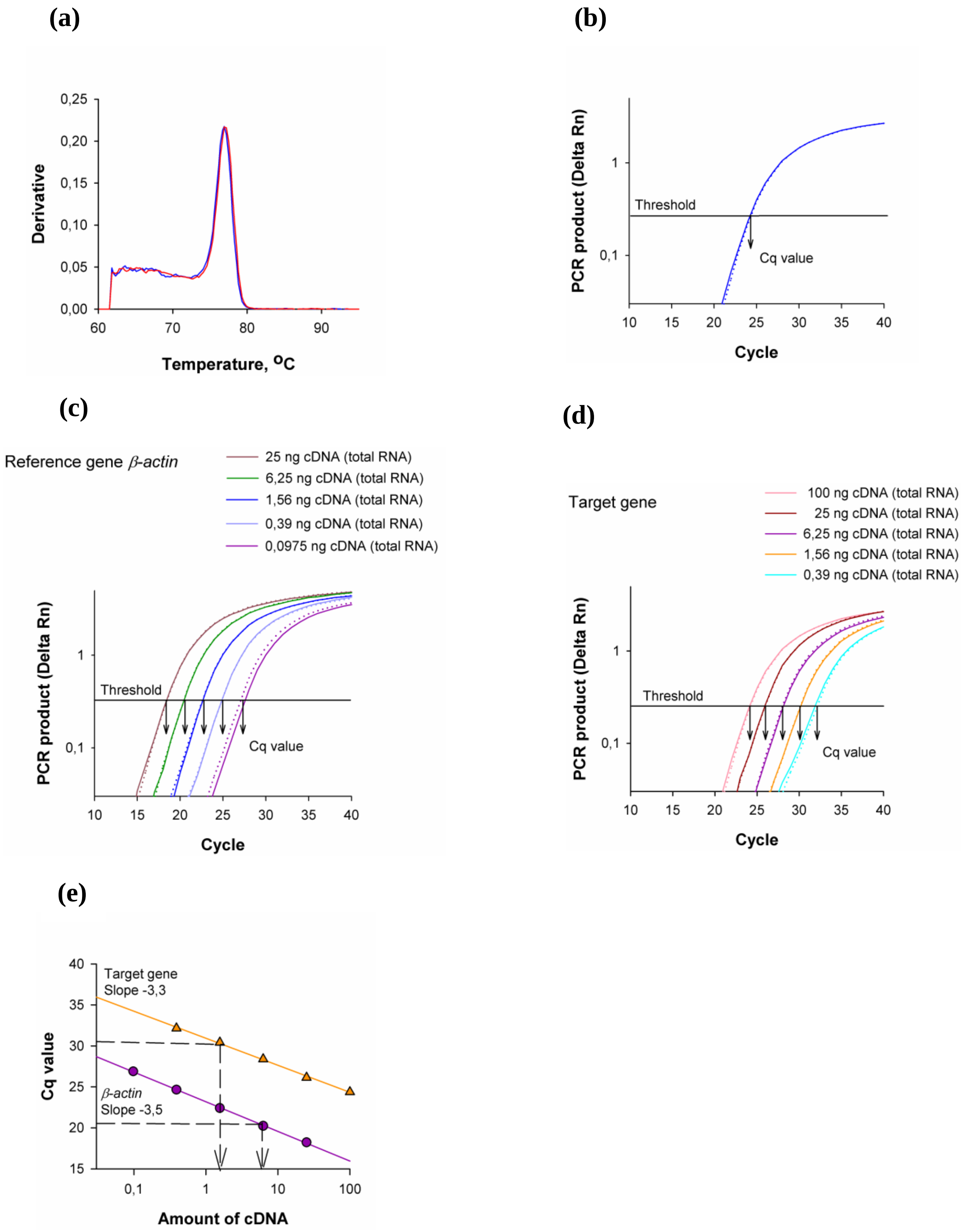

Figure 6. Quantitative polymerase chain reaction (qPCR). (a) Example of the melt curve for two samples. A single sharp peak indicates absence of byproducts. **(b)** Example of an amplification plot. The C_q (quantification cycle) value represents the number of amplification cycles required for fluorescence signals to reach a computer-defined threshold. Delta Rn equals the intensity of the fluorescence emitted by the SYBR green bound PCR product. **(c, d)** Amplification plots of the dilution series of the reference gene *β-actin* (c) and the target gene *Cckbr* (d). Dotted lines in b, c, and d represent the parallel of each concentration. **(e)** Example of quantification of gene expression by the standard curve for *β-actin* and *Cckbr*. The C_q value for each sample corresponds to a specific amount of cDNA indicated by the arrows.

3.4.6 Data analysis and statistics

Fold change values for each sample were defined by the expression of the target gene normalized to the expression of the reference gene encoding β-actin. Statistical analyses were performed on log-transformed data to compensate for non-normal distributions. Group means were compared by the use of unpaired two-tailed Student´s *t*-test.

Data are given as means ± SEM. A p-value ≤ 0.05 was chosen as the level of statistical significance.

4 Results

4.1 Positron emission tomography (PET)

Nociceptive high frequency stimulation (HFS) conditioning of the left sciatic nerve was associated with reduced supraspinal binding (HFS < baseline) of the opioid receptor (OR) agonist ligand [^{18}F]PEO. The areas involved included ipsilateral primary somatosensory cortex, visual cortex, and hippocampus. The group pretreated with MS-275 (HFS$_{MS\text{-}275}$ < baseline$_{MS\text{-}275}$) displayed less pronounced reduction in binding of tracer. Only the primary somatosensory cortex had a statistical significant reduction in tracer binding 180 min after induction of LTP in animals pretreated with MS-275. Moreover, there were no statistical significant differences in tracer binding for the intergroup comparisons (baseline vs. baseline$_{MS\text{-}275}$, and HFS relative to baseline vs. HFS$_{MS\text{-}275}$ relative to baseline $_{MS\text{-}275}$). The extracted peak T-values ($t \geq 3.747$) passing the probability threshold $p \leq 0.01$ are listed below in bold (Table 2). The HFS effect is shown by T-maps co-registered with a magnetic resonance imaging (MRI) template (Figure 7 and 8).

Table 2. T-values extracted from volumes of interest (VOI) after comparison of baseline and high frequency (HFS) conditioning (HFS < baseline, and HFS$_{MS\text{-}275}$ < baseline$_{MS\text{-}275}$). T-values passing the probability threshold of $p \leq 0.01$ ($t \geq 3.747$, 4 degrees of freedom) are shown in bold.

Region	HFS group			HFS$_{Ms\text{-}275}$ group		
	Average	Peak	Sd	Average	Peak	Sd
Ipsilateral						
Primary somatosensory cortex	4.31	**5.10**	0.70	2.39	**4.65**	0.93
Primary visual cortex	1.65	**4.65**	1.26	1.58	2.89	0.42
Lateral secondary visual cortex	2.11	**4.74**	1.45	1.82	3.44	0.65
Hippocampus – CA1	2.20	**6.28**	1.36	1.85	3.50	0.62
Hippocampus – CA2&3	2.23	**5.14**	1.15	1.78	3.23	0.41
Hippocampus – Dentate gyrus	1.78	**5.42**	1.16	1.58	2.79	0.45

Group results from [^{18}F]PEO PET study. T-values are obtained from group analysis between baseline and HFS conditioning for both groups, i.e. the HFS group and the group pretreated with MS-275 (HFS$_{Ms\text{-}275}$ group). CA: cornu ammonis, HFS: high frequency stimulation, PET: positron emission tomography.

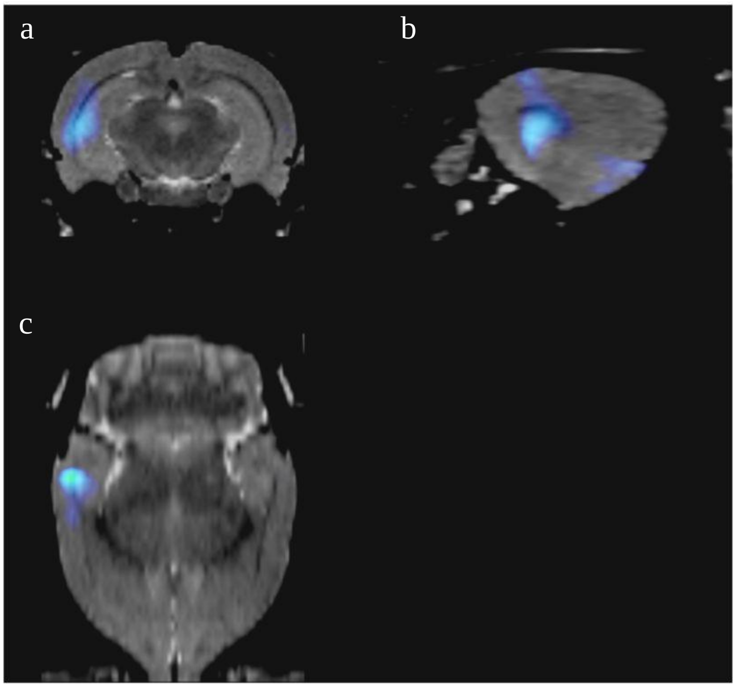

Figure 7. Regional decrease in binding of the OR agonist ligand ([18F]PEO) after comparison of baseline and HFS conditioning. The statistical significant parametric T-map (p ≤ 0.01; blue) was co-registered with a MRI template. **(a)** Coronal, **(b)** sagittal, and **(c)** axial representations of decreased tracer binding observed in rat hippocampus. Left side of the images (a and c) represents left side of the brain. HFS: high frequency stimulation, MRI: magnetic resonance imaging, OR: opioid receptor, PET: positron emission tomography.

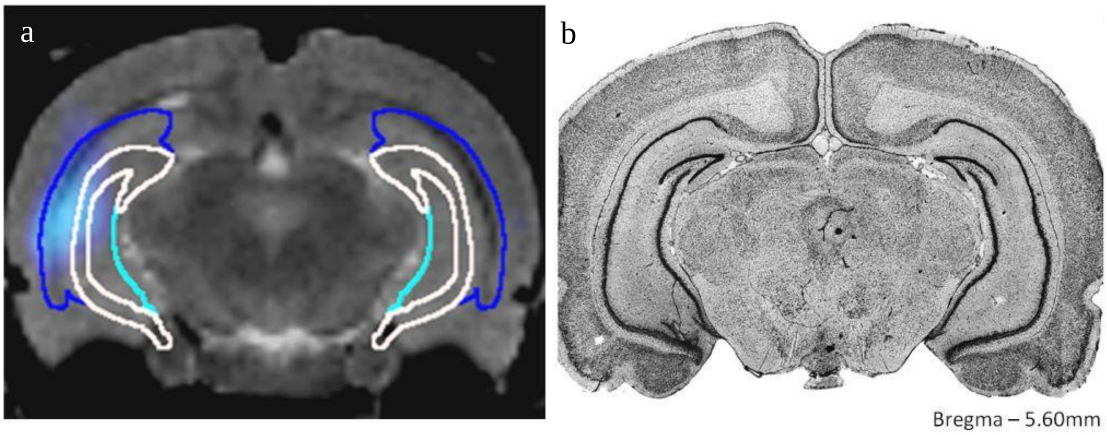

Figure 8. **Localization of regional decreased binding of the OR agonist ligand [18F]PEO after comparison of baseline and HFS conditioning. (a)** An example of how a statistical significant parametric T-map (p ≤ 0.01; blue) was co-registered with a MRI template and a 3-D digital version of "The Rat Brain in Stereotaxic Coordinates" - Paxinos & Watson (Hjornevik et al. 2007) to locate the PET signals (blue line: CA1, turquoise line: CA2&3, white line: dentate gyrus). **(b)** Histochemical representation (The rat brain - Paxinos & Watson) of a coronal section corresponding to the section shown in (a). The left side of the images represents left side of the brain. CA: cornu ammonis, HFS: high frequency stimulation, MRI: magnetic resonance imaging, OR: opioid receptor, PET: positron emission tomography.

4.2 Gene expression

Changes in gene expression of *Oprk1*, *Oprm1*, *Cckbr*, and *Penk* were investigated in tissue samples from the caudal part of the ipsilateral hippocampus in native animals, i.e. immediately after anaesthesia and without surgery, and 180 min after HFS conditioning or 180 min after sham surgery. No statistical significant changes in the level of gene expression were observed between the groups (HFS vs. control or native) for any of the genes investigated (Figure 9).

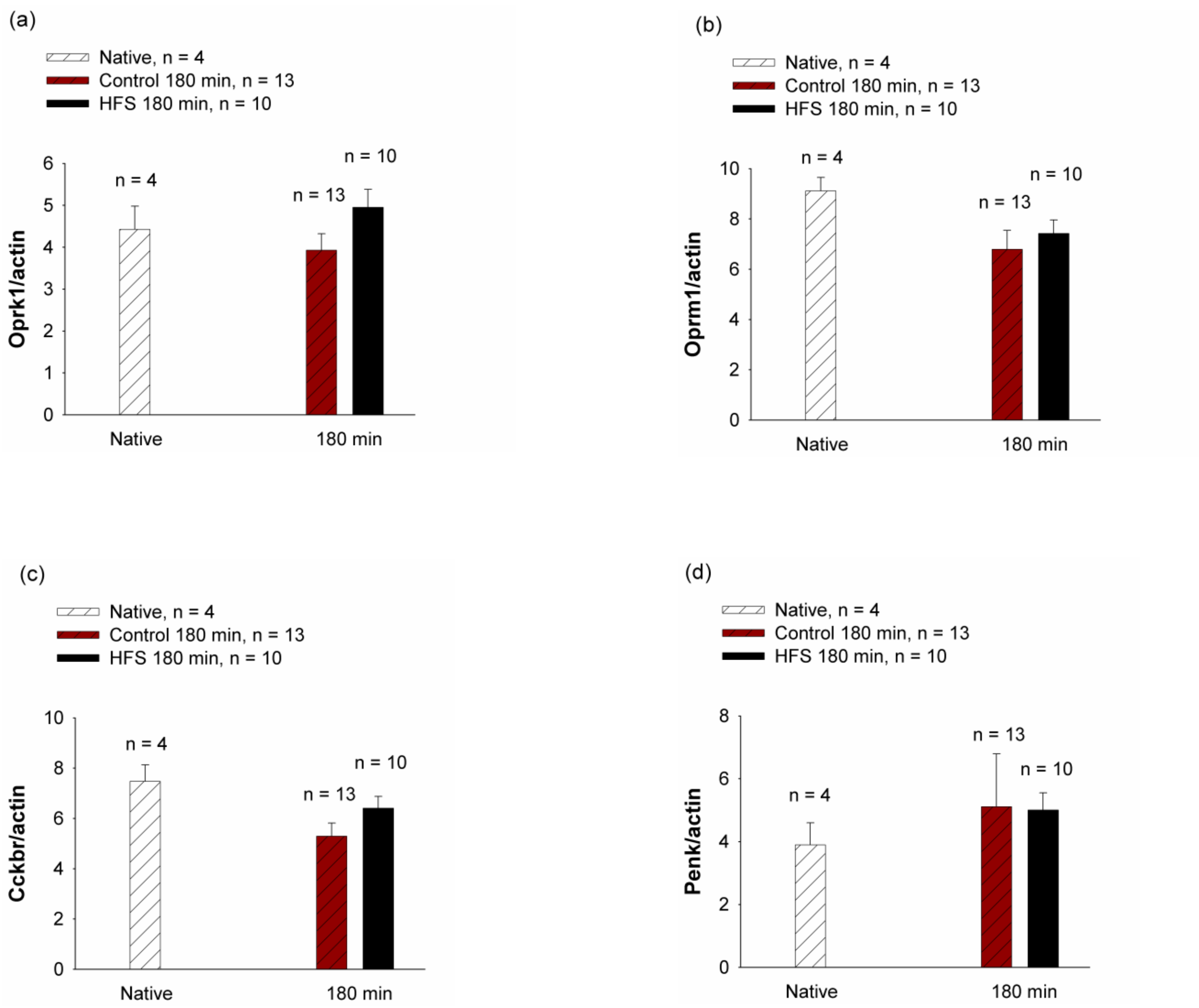

Figure 9. Gene expression analyses of ipsilateral hippocampus tissue in native animals, i.e. immediately after anaesthesia and without surgery, and 180 min HFS conditioning or 180 min after sham surgery. Gene expression in the native group, HFS group, and control group of the target genes: **(a)** *Oprk1*, **(b)** *Oprm1*, **(c)** *Cckbr*, and **(d)** *Penk* relative to the reference gene *β-actin*. Data are given as mean ± SEM. Cckbr: cholecystokinin B receptor, HFS: high frequency stimulation, Oprk1: opioid receptor kappa 1, Oprm1: opioid receptor mu 1, Penk: pre-proenkephalin.

5 Discussion of methods

5.1 Animals and anaesthesia

Sprague Dawley (SD) rats have been used extensively in positron emission tomography (PET) studies, as well as in different animal pain models, and were therefore chosen for this project (Hjornevik et al. 2008; Pedersen et al. 2010). Female SD rats were preferred over male SD rats due to the presumed lower risk for the researcher to develop allergies. However, it should be kept in mind that there might be possible sex-related differences in the nociceptive processing between female and male rats (Sandkuhler 2009).

The rats were all lightly anaesthetized by inhalation of isoflurane, which is a commonly used anaesthetic drug in recovery experiments. The induction and recovery from anaesthesia with isoflurane are rapid with no known long-lasting side effects. Furthermore, during light anaesthesia, cerebral blood flow remains unchanged, which is important for the cerebral distribution of the radioligands used in PET imaging studies. All anaesthetic drugs may have a potential effect on the opioid- and the nociceptive systems. However, isoflurane is considered to have only minor effects on the opioid receptor (OR) system (Quock and Vaughn 2005).

5.2 Drugs

There is a growing interest in epigenetic mechanisms and its potential impact on different pain states. Recently, animal pain models have demonstrated that inhibition of histone deacetylases (HDACs) may have an analgesic effect (Bai et al. 2010; Chiechio et al. 2009b; Zhang et al. 2011). Based on these findings, but also because of the limited knowledge about epigenetic modulation associated with pain, the HDAC inhibitor MS-275 was chosen for this project. It has been reported that a prolonged inhibition of HDACs is required for the induction of analgesia (Chiechio et al. 2009b). Hence, the animals were pretreated with MS-275 (3 mg/kg s.c.) dissolved in 5 % DMSO once every

24 h for 5 consecutive days. This systemic pretreatment ensured a wide distribution of the drug and possibly also epigenetic changes.

5.3 Surgery

Isolation of the sciatic nerve is an invasive procedure, which in theory could affect the neurotransmission and subsequently the endogenous opioid system. However, previous studies have demonstrated that the surgery itself does not seem to cause any altered neuronal excitability neither at the spinal level nor in the brain (Hjornevik et al. 2008; Rygh et al. 1999). Hence, the spinal LTP and the subsequent supraspinal functional changes are most likely due to the high frequency stimulation (HFS) conditioning, and not as a consequence of the surgery.

5.4 Positron emission tomography (PET)

PET is a non-invasive imaging technique that provides three-dimensional images of functional processes *in vivo* and is frequently used in clinical oncology, as well as in brain research. In recent years, PET has become a powerful tool in receptor studies. Distribution, density, and activity of receptors can be visualized by aid of specific radioligands or tracers, i.e. ligands labeled with positron emitting radionuclides (Heiss and Herholz 2006). A wide range of both selective- and nonselective tracers have now been synthesized for various receptor systems, including the OR system.

Previous studies have demonstrated that the OR agonist radioligand [^{11}C]PEO binds with high affinity to μ-ORs and κ-ORs, and with low affinity to the δ-ORs. Hence, [^{11}C]PEO is considered to be a selective μ- and κ- OR agonist ligand (Hjornevik et al. 2010; Marton et al. 2009). However, due to the relative short half-life of ^{11}C labelled radioligands ($t½$ = 20.3 min) (Henriksen and Willoch 2008), considerable efforts have been made to synthesize ^{18}F labelled OR agonist radioligands, which compared to ^{11}C, has a substantial longer half-life (^{18}F : $t½$ = 109.7 min) (Henriksen and Willoch 2008). In the present study the new OR agonist ligand [^{18}F]PEO was applied to investigate functional changes in the supraspinal OR system after induction of LTP.

Affinity studies have recently indicated that $[^{18}F]$PEO exhibit some altered receptor binding properties compared to the previously used $[^{11}C]$PEO. $[^{18}F]$PEO binds, as $[^{11}C]$PEO, with high affinity to both μ-ORs and κ-ORs, but $[^{18}F]$PEO also displays an enhanced affinity to the δ-ORs compared to $[^{11}C]$PEO (Schoultz et al. 2012).

The PET images of opioid tracer distribution in the present study exhibit the total radioactivity in different brain regions. Hence, the signals detected contain contributions from both specific- and nonspecific binding, as well as free ligands in tissue and intravascular activity (Henriksen and Willoch 2008). In order to determine the contribution of the various components and thus quantify the specific receptor binding, kinetic analysis has to be performed. Such analysis was, however, not performed in this study. Hence, the results display a change in tracer distribution and not a regional alteration in specific receptor binding. However, it is reasonable to assume that the nonspecific binding and the amount of free tracer in tissues are similar in both test conditions, i.e. at rest (baseline) and subsequent to the intervention (HFS-conditioning).

PET images provide limited structural information, and the assignment of anatomical location to functional effects is critical in the interpretation and the analysis of the PET images (Schwarz et al. 2006). Hence, PET is usually combined with imaging techniques providing localization and anatomical details. Magnetic resonance imaging (MRI) is commonly used for this purpose due to its high spatial resolution. Ideally, it should have been performed MRI scans of each individual animal. However, the PET images were co-registered with an in-house MRI template. Even though this is a frequently used approach in small animal PET studies, it might be susceptible to errors caused by individual anatomical differences.

5.5 Gene expression analysis

Based on the observations made in the PET study, reverse transcription quantitative polymerase chain reaction (RT-qPCR) was applied to investigate the gene expression of *Oprm1, Oprk1, Penk*, and *Cckbr* in the caudal part of the ipsilateral hippocampus. The genes were selected due to their potential role regarding the endogenous opioid system. It is believed that the underlying mechanisms of functional changes may be reflected at the level of transcription, and subsequently the mRNA concentration. However, it has to be kept in mind that an altered mRNA concentration provides no information on whether that mRNA will be translated into a functional protein.

RT-qPCR has in the last years become the method of choice for quantification of mRNA due to the combination of a relatively high sensitivity and specificity at a low cost (Bustin et al. 2005). Even though it is often described as a “gold standard”, it is far from being a standardized method (Nolan et al. 2006). Hence, there are a number of factors to be considered that may influence the reliability and the reproducibility of the results.

In this project, gene expression analyses were performed on RNA isolated from a 2 mm section of the caudal part of the ipsilateral hippocampus. Tissue harvesting and RNA isolation are critical steps of RT-qPCR preparation and may have a substantial impact on the RNA quality, and consequently the reliability and reproducibility of the results. RNA molecules are extremely fragile once removed from its cellular environment, and are continuously exposed to degradation by RNAses as well as contamination throughout the process. Utilizing degraded RNA in RT-qPCR, or a sample contaminated by e.g. inhibitors, may lead to a falsely high quantification cycle (C_q) value and subsequently underestimation of the target concentration and copy number (Bustin 2010). In contrast, DNA contamination may lead to an overestimation of target concentration and copy number.

Hence, the purity and the RNA concentration of the samples were checked and estimated spectrophotometrically by measuring the UV absorption at 260 nm, 280 nm and 230 nm. While RNA has its absorption maximum at 260 nm in a neutral buffer, proteins and phenols have their absorption maximum around 280 nm and 230 nm, respectively.

Consequently, the estimation of the optical density (OD) ration of 260 nm/280 nm ($OD_{260/280}$) and 260 nm/230 nm ($OD_{260/230}$) give an indication of the purity of the samples. Both $OD_{260/280}$ ratio and $OD_{260/230}$ ratio should be close to 2.0 in pure samples. However, this method gives limited information about the integrity of the RNA.

The RNA quality was therefore further evaluated by aid of Agilent 2100 Bioanalyzer. Agilent 2100 Bioanalyzer is an automated lab-on-chip gel electrophoresis method that utilizes fluorescent dye to determine both RNA concentration and integrity. Since messenger RNA (mRNA) comprises only about 1-3 % of total RNA in a sample, it is not easily detectable. Hence, the calculations done by Agilent 2100 Bioanalyzer were based on the ribosomal RNA (rRNA) subunits 28S and 18S. To infer the RNA quality, the software generated a RNA Integrity Number (RIN) value. The RIN value ranges from 1 to 10 where 1 is degraded and 10 is intact RNA (Schroeder et al. 2006). A RIN value equal to 7 or higher was considered to be satisfactory for RT-qPCR.

In a gene expression study, the reliability of the results is also dependent on the primers used in the qPCR reaction. Hairpin structures, primer dimers, different melting temperature (T_m) of the primers, mismatch between primer and target cDNA, and amplification of genomic DNA contamination may have a huge impact on the efficacy of the qPCR reaction and consequently the reliability of the results. To optimize the primers, and thereby limit the risk of such incidents, there are some rules that are thought to be of assistance and thus should be considered; the primer pair should be about 18-25 bases long with GC (guanine/cytosine) content in the range of 40 to 60 %. The GC content of the 3´ends is particularly important since high levels may lead to false priming. Moreover, the T_m of the primers should be between 58-60 °C and not differ more than 1-2 °C. All primers used in this project were within these parameters, except the Cckbr forward primer which had a GC content of 63.2 %. Furthermore, in this project, the primers were designed to span introns to avoid amplification of possible genomic DNA contamination and subsequent false positive results. The primer specificity was finally evaluated by BLAST search. Ideally, the specificity should also have been evaluated empirically by DNA sequencing, however this was not performed in the present study.

The qPCR efficiency was evaluated by a 4-fold serial dilution of known concentration accompanied with generation of an amplification plot and a standard curve. The maximum increase of amplicon per cycle is 2-fold (100 % efficient), corresponding to a slope equal to -3.32 on the standard curve. Reactions with low efficiency (< 90 %) may be due to contamination by inhibitors, suboptimal annealing temperature, amplicons with secondary structures or low primer concentration. High efficiency (> 110 %), on the other hand, may originate from unspecific priming or primer dimers, which may result from poorly designed primers or too high primer concentration (Taylor et al. 2010).

Moreover, melt curve analysis was performed at the end of each qPCR run. A melt curve, i.e. fluorescence as function of temperature, displays the T_m of the amplified product and depends on both the product size and the nucleotide composition. Hence, each amplicon has a characteristic T_m. Based on the melt curve analyses in this study, no byproducts were observed for either of the genes. However, some byproducts could theoretically have T_m close to the target amplicon. Gel electrophoresis should therefore have been performed to confirm that there was only one amplicon.

All results obtained from a RT-qPCR assay are subject to variability caused by technical as well as biological variation (Nolan et al. 2006). These variabilities may include differences in gene expression levels between the animals, differences in the amount or quality of the starting material, and differences in sample quality and quantity caused by differences in the RNA isolation and the cDNA synthesis (Radonic et al. 2004; Taylor et al. 2010). To mitigate the effect of the technical variations, the mRNA level of each sample was normalized to a reference gene, which was co-amplified with the target gene. A good reference gene should have a constant expression in all samples included in the study and should not be influenced by the experimental manipulations performed (Radonic et al. 2004). Ideally, more than one reference gene should be included in the assay (Bustin et al. 2009). In this project, the gene encoding β-actin was selected as a reference gene in accordance with previous gene expression studies on spinal cord and brain (Pedersen et al. 2010; Tanic et al. 2007). β-actin is a ubiquitous cytoskeleton protein and the gene expression is therefore most likely unaffected by the interventions used in this study.

6 Discussion of results

6.1 Positron emission tomography (PET)

The present study demonstrated that induction of spinal long-term potentiation (LTP) by high frequency stimulation (HFS) conditioning was associated with a reduced opioid tracer binding, i.e. reduced receptor availability, in the ipsilateral primary somatosensory cortex, visual cortex, and hippocampus. These findings suggest that a peripheral noxious stimulation may activate the supraspinal opioid receptor (OR) system, especially in the hippocampus. The observed decrease in opioid tracer binding is most likely explained by an increase in the endogenous opioid peptide release. However, a downregulation or internalization of the ORs cannot be excluded. Based on the findings, the main focus in this study was on hippocampus and its prospective role in nociceptive processing.

Hippocampus is an integral part of the limbic system with connections to thalamus, hypothalamus, amygdala, as well as entorhinal cortex (Bird and Burgess 2008). Its functional role in learning and memory is now well established (Bird and Burgess 2008; Eichenbaum 2000). However, hippocampus as a part of the pain processing brain network is still a matter of debate. Although its functional role regarding nociceptive processing is yet not clear, the data in the present study may support previous findings suggesting that an activation of the endogenous opioid system in hippocampus might have an antinociceptive effect (Erfanparast et al. 2010; Favaroni Mendes and Menescal-de-Oliveira 2008) which may occur through inhibition of tonically active GABAergic interneurons (Favaroni Mendes and Menescal-de-Oliveira 2008).

It has earlier been demonstrated that ORs are widely distributed in the hippocampus (Mansour et al. 1995; McLean et al. 1987) and are found on GABAergic interneurons. Activation of these ORs may lead to an inhibition of the GABAergic interneurons (Madison and Nicoll 1988; Wimpey and Chavkin 1991) and subsequent reduction of GABA release. GABA can have an inhibitory effect on the hippocampal pyramidal cells

(Cohen et al. 1992; Svoboda and Lupica 1998). Hence, a potential inhibition of the GABAergic interneurons may lead to a disinhibition of the hippocampal pyramidal cells.

Previous PET studies investigating the endogenous OR system report findings in brain structures such as nucleus accumbens, hypothalamus, anterior cingulate cortex, insular cortex, thalamus, and amygdala (Hjornevik et al. 2010; Zubieta et al. 2001), but not in the hippocampus. However, pain is a complex experience comprising sensory, cognitive, and emotional components. Thus, it is reasonable to believe that hippocampus, as a part of the limbic system, is involved in the pain processing brain network. In fact, there are several lines of evidence, with different approaches, indicating such involvement (Al Amin et al. 2004; Echeverry et al. 2004; Favaroni Mendes and Menescal-de-Oliveira 2008; Khanna et al. 2004; McKenna and Melzack 1992; Schneider et al. 2001; Shih et al. 2008; Zhao et al. 2009).

However, it has to be emphasized that both methodological- and individual variabilities may have a considerable impact on the results and consequently the conclusions presented. In the present study, a new opioid tracer ([^{18}F]PEO) was introduced, and a substantial uptake of the tracer by the cranium was observed. This nonspecific tracer binding and subsequent enhanced background noise may have an impact on the analyses of the data and thereby the interpretation of the results.

As a part of this PET study, a group of animals were pretreated with the histone deacetaylase (HDAC) inhibitor MS-275 prior to the induction of spinal LTP. Previous findings have suggested that inhibition of HDACs may have an analgesic effect through acetylation and subsequent prolonged activation of the transcription factor nuclear factor κB (NF-κB) (Chiechio et al. 2009b). Activation of NF-κB may promote transcription of NF-κB regulated genes including genes encoding metabotropic glutamate 2 and 3 (mGlu2/3) receptors (Chiechio et al. 2009a). It has been suggested that activation of mGlu2/3 receptors on the central terminalis of the primary afferent neurons may have an antinociceptive effect through inhibition of spinal dorsal horn glutamate release and consequently inhibition of the spinal nociceptive signaling (Dolan and Nolan 2000; Gerber et al. 2000), for reviews see (Goudet et al. 2009; Niswender and Conn 2010). Hence, it is tempting to speculate that the antinociceptive effect caused by inhibition of

HDACs may affect the supraspinal nociceptive processing due to the diminished nociceptive spinal signaling. If this was the case, a reduced activation of supraspinal opioid neurotransmission after HFS conditioning could be expected in the MS-275 pretreated animals. However, the results obtained in this study showed only an overall tendency of reduced activation of the endogenous OR system compared with the untreated animals. Hence, only a minor effect of the HDAC inhibitor on the OR system was observed.

6.2 Gene expression

Experimental neuropathic pain has earlier been associated with a decreased OR mRNA expression in the dorsal root ganglia in rats (Obara et al. 2009). Furthermore, the expression of pre-proenkephalin mRNA has been demonstrated to be elevated during inflammatory pain (Noguchi et al. 1992). Similar mechanisms could also be relevant for the changed supraspinal opioid activity observed in the present PET study. Hence, the genes: *Oprm1, Oprk1,* and *Penk* were chosen to be further investigated due to their potential involvement in the observed reduction in OR availability.

The OR availability may be influenced by several factors including the amount of receptors at the cell surface. Both downregulation of the ORs and receptor internalization could explain a reduction in total tracer binding. Moreover, the endogenous opioid peptides and the agonistic opioid tracer would compete for the same receptor binding sites. Hence, available binding sites decrease by an increased occupancy of endogenous opioid peptides.

No change in mRNA expression was observed for the genes encoding OR-μ, OR-κ, or pre-proenkephalin. It has previously been demonstrated that peripheral nerve injuries alter the CCK_B receptor mRNA expression in rat dorsal root ganglion (Zhang et al. 1993). Still, no such change was observed for the mRNA expression of *Cckbr* in the ipsilateral hippocampus.

However, OR internalization would not necessarily be detected at the mRNA level. Furthermore, the endogenous opioid peptides may be stored in dense-core vesicles in the terminals of the neurons. An increased endogenous opioid peptide release could therefore be explained by an enhanced activation and subsequent release from these intracellular stores and not by *de novo* protein synthesis.

7 Conclusions

I) A supraspinal decrease in opioid tracer binding was observed 180 min after HFS conditioning. These findings suggest that induction of spinal LTP may be associated with increased supraspinal opioid neurotransmission, especially in the hippocampus.

II) No pronounced changes of opioid tracer binding were observed in animals pretreated with the HDAC inhibitor MS-275, neither at rest nor 180 min after HFS conditioning.

III) No clear changes in the gene expression of *Oprm1*, *Oprk1*, *Penk*, or *Cckbr* in the ipsilateral hippocampus were observed 180 min after HFS conditioning.

8 References

Al Amin, H.A., Atweh, S.F., Jabbur, S.J. and Saade, N.E., Effects of ventral hippocampal lesion on thermal and mechanical nociception in neonates and adult rats, Eur J Neurosci, 20 (2004) 3027-34.

Ashburner, B.P., Westerheide, S.D. and Baldwin, A.S., Jr., The p65 (RelA) subunit of NF-kappaB interacts with the histone deacetylase (HDAC) corepressors HDAC1 and HDAC2 to negatively regulate gene expression, Mol Cell Biol, 21 (2001) 7065-77.

Azkue, J.J., Mateos, J.M., Elezgarai, I., Benitez, R., Osorio, A., Diez, J., Bilbao, A., Bidaurrazaga, A. and Grandes, P., The metabotropic glutamate receptor subtype mGluR 2/3 is located at extrasynaptic loci in rat spinal dorsal horn synapses, Neurosci Lett, 287 (2000) 236-8.

Bai, G., Wei, D., Zou, S., Ren, K. and Dubner, R., Inhibition of class II histone deacetylases in the spinal cord attenuates inflammatory hyperalgesia, Mol Pain, 6 (2010) 51.

Barrett, R.M. and Wood, M.A., Beyond transcription factors: the role of chromatin modifying enzymes in regulating transcription required for memory, Learn Mem, 15 (2008) 460-7.

Bederson, J.B., Fields, H.L. and Barbaro, N.M., Hyperalgesia during naloxone-precipitated withdrawal from morphine is associated with increased on-cell activity in the rostral ventromedial medulla, Somatosens Mot Res, 7 (1990) 185-203.

Beitz, A.J., The organization of afferent projections to the midbrain periaqueductal gray of the rat, Neuroscience, 7 (1982) 133-59.

Bie, B. and Pan, Z.Z., Presynaptic mechanism for anti-analgesic and anti-hyperalgesic actions of kappa-opioid receptors, J Neurosci, 23 (2003) 7262-8.

Bird, C.M. and Burgess, N., The hippocampus and memory: insights from spatial processing, Nat Rev Neurosci, 9 (2008) 182-94.

Bliss, T.V. and Lomo, T., Long-lasting potentiation of synaptic transmission in the dentate area of the anaesthetized rabbit following stimulation of the perforant path, J Physiol, 232 (1973) 331-56.

Burstein, R., Cliffer, K.D. and Giesler, G.J., Jr., Direct somatosensory projections from the spinal cord to the hypothalamus and telencephalon, J Neurosci, 7 (1987) 4159-64.

Bustin, S.A., Why the need for qPCR publication guidelines?--The case for MIQE, Methods, 50 (2010) 217-26.

Bustin, S.A., Benes, V., Garson, J.A., Hellemans, J., Huggett, J., Kubista, M., Mueller, R., Nolan, T., Pfaffl, M.W., Shipley, G.L., Vandesompele, J. and Wittwer, C.T., The MIQE guidelines: minimum information for publication of quantitative real-time PCR experiments, Clin Chem, 55 (2009) 611-22.

Bustin, S.A., Benes, V., Nolan, T. and Pfaffl, M.W., Quantitative real-time RT-PCR--a perspective, J Mol Endocrinol, 34 (2005) 597-601.

Carlton, S.M., Du, J. and Zhou, S., Group II metabotropic glutamate receptor activation on peripheral nociceptors modulates TRPV1 function, Brain Res, 1248 (2009) 86-95.

Carlton, S.M., Hargett, G.L. and Coggeshall, R.E., Localization of metabotropic glutamate receptors 2/3 on primary afferent axons in the rat, Neuroscience, 105 (2001) 957-69.

Chavkin, C., James, I.F. and Goldstein, A., Dynorphin is a specific endogenous ligand of the kappa opioid receptor, Science, 215 (1982) 413-5.

Chen, L. and Huang, L.Y., Protein kinase C reduces Mg2+ block of NMDA-receptor channels as a mechanism of modulation, Nature, 356 (1992) 521-3.

Chiechio, S., Copani, A., Zammataro, M., Battaglia, G., Gereau, R.W.t. and Nicoletti, F., Transcriptional regulation of type-2 metabotropic glutamate receptors: an epigenetic path to novel treatments for chronic pain, Trends Pharmacol Sci, 31 (2009a) 153-60.

Chiechio, S., Zammataro, M., Morales, M.E., Busceti, C.L., Drago, F., Gereau, R.W.t., Copani, A. and Nicoletti, F., Epigenetic modulation of mGlu2 receptors by histone deacetylase inhibitors in the treatment of inflammatory pain, Mol Pharmacol, 75 (2009b) 1014-20.

Cohen, G.A., Doze, V.A. and Madison, D.V., Opioid inhibition of GABA release from presynaptic terminals of rat hippocampal interneurons, Neuron, 9 (1992) 325-35.

Crawley, J.N. and Corwin, R.L., Biological actions of cholecystokinin, Peptides, 15 (1994) 731-55.

D'Mello, R. and Dickenson, A.H., Spinal cord mechanisms of pain, Br J Anaesth, 101 (2008) 8-16.

Dolan, S. and Nolan, A.M., Behavioural evidence supporting a differential role for group I and II metabotropic glutamate receptors in spinal nociceptive transmission, Neuropharmacology, 39 (2000) 1132-8.

Dutar, P., Vu, H.M. and Perkel, D.J., Pharmacological characterization of an unusual mGluR-evoked neuronal hyperpolarization mediated by activation of GIRK channels, Neuropharmacology, 38 (1999) 467-75.

Echeverry, M.B., Guimaraes, F.S. and Del Bel, E.A., Acute and delayed restraint stress-induced changes in nitric oxide producing neurons in limbic regions, Neuroscience, 125 (2004) 981-93.

Eichenbaum, H., A cortical-hippocampal system for declarative memory, Nat Rev Neurosci, 1 (2000) 41-50.

Erfanparast, A., Tamaddonfard, E., Farshid, A.A. and Khalilzadeh, E., Effect of microinjection of histamine into the dorsal hippocampus on the orofacial formalin-induced pain in rats, Eur J Pharmacol, 627 (2010) 119-23.

Faris, P.L., Komisaruk, B.R., Watkins, L.R. and Mayer, D.J., Evidence for the neuropeptide cholecystokinin as an antagonist of opiate analgesia, Science, 219 (1983) 310-2.

Favaroni Mendes, L.A. and Menescal-de-Oliveira, L., Role of cholinergic, opioidergic and GABAergic neurotransmission of the dorsal hippocampus in the modulation of nociception in guinea pigs, Life Sci, 83 (2008) 644-50.

Felsenfeld, G. and Groudine, M., Controlling the double helix, Nature, 421 (2003) 448-53.

Fields, H.L. and Heinricher, M.M., Anatomy and physiology of a nociceptive modulatory system, Philos Trans R Soc Lond B Biol Sci, 308 (1985) 361-74.

Foo, H. and Mason, P., Discharge of raphe magnus ON and OFF cells is predictive of the motor facilitation evoked by repeated laser stimulation, J Neurosci, 23 (2003) 1933-40.

Gerber, G., Zhong, J., Youn, D. and Randic, M., Group II and group III metabotropic glutamate receptor agonists depress synaptic transmission in the rat spinal cord dorsal horn, Neuroscience, 100 (2000) 393-406.

Gerber, U. and Gahwiler, B.H., Modulation of potassium conductances by metabotropic glutamate receptors in the hippocampus, Ren Physiol Biochem, 17 (1994) 129-31.

Gjerstad, J., Genetic susceptibility and development of chronic non-malignant back pain, Rev Neurosci, 18 (2007) 83-91.

Glozak, M.A., Sengupta, N., Zhang, X. and Seto, E., Acetylation and deacetylation of non-histone proteins, Gene, 363 (2005) 15-23.

Goudet, C., Magnaghi, V., Landry, M., Nagy, F., Gereau, R.W.t. and Pin, J.P., Metabotropic receptors for glutamate and GABA in pain, Brain Res Rev, 60 (2009) 43-56.

Gray, A.C., Coupar, I.M. and White, P.J., Comparison of opioid receptor distributions in the rat central nervous system, Life Sci, 79 (2006) 674-85.

Hardy, S.G. and Leichnetz, G.R., Frontal cortical projections to the periaqueductal gray in the rat: a retrograde and orthograde horseradish peroxidase study, Neurosci Lett, 23 (1981) 13-7.

Heinricher, M.M., Barbaro, N.M. and Fields, H.L., Putative nociceptive modulating neurons in the rostral ventromedial medulla of the rat: firing of on- and off-cells is related to nociceptive responsiveness, Somatosens Mot Res, 6 (1989) 427-39.

Heinricher, M.M., McGaraughty, S. and Tortorici, V., Circuitry underlying antiopioid actions of cholecystokinin within the rostral ventromedial medulla, J Neurophysiol, 85 (2001) 280-6.

Heinricher, M.M. and Neubert, M.J., Neural basis for the hyperalgesic action of cholecystokinin in the rostral ventromedial medulla, J Neurophysiol, 92 (2004) 1982-9.

Heiss, W.D. and Herholz, K., Brain receptor imaging, J Nucl Med, 47 (2006) 302-12.

Henriksen, G. and Willoch, F., Imaging of opioid receptors in the central nervous system, Brain, 131 (2008) 1171-96.

Hjornevik, T., Jacobsen, L.M., Qu, H., Bjaalie, J.G., Gjerstad, J. and Willoch, F., Metabolic plasticity in the supraspinal pain modulating circuitry after noxious stimulus-induced spinal cord LTP, Pain, 140 (2008) 456-64.

Hjornevik, T., Leergaard, T.B., Darine, D., Moldestad, O., Dale, A.M., Willoch, F. and Bjaalie, J.G., Three-dimensional atlas system for mouse and rat brain imaging data, Front Neuroinform, 1 (2007) 4.

Hjornevik, T., Schoultz, B.W., Marton, J., Gjerstad, J., Drzezga, A., Henriksen, G. and Willoch, F., Spinal long-term potentiation is associated with reduced opioid neurotransmission in the rat brain, Clin Physiol Funct Imaging, 30 (2010) 285-93.

Hopkins, D.A. and Holstege, G., Amygdaloid projections to the mesencephalon, pons and medulla oblongata in the cat, Exp Brain Res, 32 (1978) 529-47.

Hylden, J.L., Anton, F. and Nahin, R.L., Spinal lamina I projection neurons in the rat: collateral innervation of parabrachial area and thalamus, Neuroscience, 28 (1989) 27-37.

Ikeda, K., Kobayashi, T., Kumanishi, T., Yano, R., Sora, I. and Niki, H., Molecular mechanisms of analgesia induced by opioids and ethanol: is the GIRK channel one of the keys?, Neurosci Res, 44 (2002) 121-131.

Ji, R.R., Baba, H., Brenner, G.J. and Woolf, C.J., Nociceptive-specific activation of ERK in spinal neurons contributes to pain hypersensitivity, Nat Neurosci, 2 (1999) 1114-9.

Jia, H., Rustioni, A. and Valtschanoff, J.G., Metabotropic glutamate receptors in superficial laminae of the rat dorsal horn, J Comp Neurol, 410 (1999) 627-42.

Jones, S.L. and Gebhart, G.F., Characterization of coeruleospinal inhibition of the nociceptive tail-flick reflex in the rat: mediation by spinal alpha 2-adrenoceptors, Brain Res, 364 (1986) 315-30.

Khanna, S., Chang, L.S., Jiang, F. and Koh, H.C., Nociception-driven decreased induction of Fos protein in ventral hippocampus field CA1 of the rat, Brain Res, 1004 (2004) 167-76.

Kieffer, B.L., Recent advances in molecular recognition and signal transduction of active peptides: receptors for opioid peptides, Cell Mol Neurobiol, 15 (1995) 615-35.

Kieffer, B.L. and Evans, C.J., Opioid receptors: from binding sites to visible molecules in vivo, Neuropharmacology, 56 Suppl 1 (2009) 205-12.

Kieffer, B.L. and Gaveriaux-Ruff, C., Exploring the opioid system by gene knockout, Prog Neurobiol, 66 (2002) 285-306.

Kim, J.S., Lee, J.S., Im, K.C., Kim, S.J., Kim, S.Y., Lee, D.S. and Moon, D.H., Performance measurement of the microPET focus 120 scanner, J Nucl Med, 48 (2007) 1527-35.

Knoflach, F. and Kemp, J.A., Metabotropic glutamate group II receptors activate a G protein-coupled inwardly rectifying K+ current in neurones of the rat cerebellum, J Physiol, 509 (Pt 2) (1998) 347-54.

Kovelowski, C.J., Ossipov, M.H., Sun, H., Lai, J., Malan, T.P. and Porreca, F., Supraspinal cholecystokinin may drive tonic descending facilitation mechanisms to maintain neuropathic pain in the rat, Pain, 87 (2000) 265-73.

Kritzer, M.F., Innis, R.B. and Goldman-Rakic, P.S., Regional distribution of cholecystokinin receptors in macaque medial temporal lobe determined by in vitro receptor autoradiography, J Comp Neurol, 276 (1988) 219-30.

Lai, J., Luo, M.C., Chen, Q., Ma, S., Gardell, L.R., Ossipov, M.H. and Porreca, F., Dynorphin A activates bradykinin receptors to maintain neuropathic pain, Nat Neurosci, 9 (2006) 1534-40.

Latremoliere, A. and Woolf, C.J., Central sensitization: a generator of pain hypersensitivity by central neural plasticity, J Pain, 10 (2009) 895-926.

Laughlin, T.M., Larson, A.A. and Wilcox, G.L., Mechanisms of induction of persistent nociception by dynorphin, J Pharmacol Exp Ther, 299 (2001) 6-11.

Laughlin, T.M., Vanderah, T.W., Lashbrook, J., Nichols, M.L., Ossipov, M., Porreca, F. and Wilcox, G.L., Spinally administered dynorphin A produces long-lasting allodynia: involvement of NMDA but not opioid receptors, Pain, 72 (1997) 253-60.

Li, Y. and Han, J.S., Cholecystokinin-octapeptide antagonizes morphine analgesia in periaqueductal gray of the rat, Brain Res, 480 (1989) 105-10.

Light, A.R. and Perl, E.R., Spinal termination of functionally identified primary afferent neurons with slowly conducting myelinated fibers, J Comp Neurol, 186 (1979) 133-50.

Lin, Q., Peng, Y.B. and Willis, W.D., Possible role of protein kinase C in the sensitization of primate spinothalamic tract neurons, J Neurosci, 16 (1996) 3026-34.

Lin, Q., Wu, J. and Willis, W.D., Effects of protein kinase a activation on the responses of primate spinothalamic tract neurons to mechanical stimuli, J Neurophysiol, 88 (2002) 214-21.

Liu, X.G. and Sandkuhler, J., Long-term potentiation of C-fiber-evoked potentials in the rat spinal dorsal horn is prevented by spinal N-methyl-D-aspartic acid receptor blockage, Neurosci Lett, 191 (1995) 43-6.

Loeser, J.D. and Treede, R.D., The Kyoto protocol of IASP Basic Pain Terminology, Pain, 137 (2008) 473-7.

Lovick, T.A., Pro-nociceptive action of cholecystokinin in the periaqueductal grey: a role in neuropathic and anxiety-induced hyperalgesic states, Neurosci Biobehav Rev, 32 (2008) 852-62.

Ma, J.Y. and Zhao, Z.Q., The involvement of glia in long-term plasticity in the spinal dorsal horn of the rat, Neuroreport, 13 (2002) 1781-4.

Madison, D.V. and Nicoll, R.A., Enkephalin hyperpolarizes interneurones in the rat hippocampus, J Physiol, 398 (1988) 123-30.

Mansour, A., Fox, C.A., Akil, H. and Watson, S.J., Opioid-receptor mRNA expression in the rat CNS: anatomical and functional implications, Trends Neurosci, 18 (1995) 22-9.

Martin, W.R., Eades, C.G., Thompson, J.A., Huppler, R.E. and Gilbert, P.E., The effects of morphine- and nalorphine- like drugs in the nondependent and morphine-dependent chronic spinal dog, J Pharmacol Exp Ther, 197 (1976) 517-32.

Marton, J., Schoultz, B.W., Hjornevik, T., Drzezga, A., Yousefi, B.H., Wester, H.J., Willoch, F. and Henriksen, G., Synthesis and evaluation of a full-agonist orvinol for PET-imaging of opioid receptors: [11C]PEO, J Med Chem, 52 (2009) 5586-9.

McKenna, J.E. and Melzack, R., Analgesia produced by lidocaine microinjection into the dentate gyrus, Pain, 49 (1992) 105-12.

McLean, S., Rothman, R.B., Jacobson, A.E., Rice, K.C. and Herkenham, M., Distribution of opiate receptor subtypes and enkephalin and dynorphin immunoreactivity in the hippocampus of squirrel, guinea pig, rat, and hamster, J Comp Neurol, 255 (1987) 497-510.

McMahon, S.B., Cafferty, W.B. and Marchand, F., Immune and glial cell factors as pain mediators and modulators, Exp Neurol, 192 (2005) 444-62.

Meng, I.D., Johansen, J.P., Harasawa, I. and Fields, H.L., Kappa opioids inhibit physiologically identified medullary pain modulating neurons and reduce morphine antinociception, J Neurophysiol, 93 (2005) 1138-44.

Mercer, L.D., Le, V.Q., Nunan, J., Jones, N.M. and Beart, P.M., Direct visualization of cholecystokinin subtype2 receptors in rat central nervous system using anti-peptide antibodies, Neurosci Lett, 293 (2000) 167-70.

Millan, M.J., Descending control of pain, Prog Neurobiol, 66 (2002) 355-474.

Milligan, E.D. and Watkins, L.R., Pathological and protective roles of glia in chronic pain, Nat Rev Neurosci, 10 (2009) 23-36.

Mills, C.D., Johnson, K.M. and Hulsebosch, C.E., Role of group II and group III metabotropic glutamate receptors in spinal cord injury, Exp Neurol, 173 (2002) 153-67.

Moran, T.H., Robinson, P.H., Goldrich, M.S. and McHugh, P.R., Two brain cholecystokinin receptors: implications for behavioral actions, Brain Res, 362 (1986) 175-9.

Niswender, C.M. and Conn, P.J., Metabotropic glutamate receptors: physiology, pharmacology, and disease, Annu Rev Pharmacol Toxicol, 50 (2010) 295-322.

Noble, F. and Roques, B.P., CCK-B receptor: chemistry, molecular biology, biochemistry and pharmacology, Prog Neurobiol, 58 (1999) 349-79.

Noguchi, K., Dubner, R. and Ruda, M.A., Preproenkephalin mRNA in spinal dorsal horn neurons is induced by peripheral inflammation and is co-localized with Fos and Fos-related proteins, Neuroscience, 46 (1992) 561-70.

Nolan, T., Hands, R.E. and Bustin, S.A., Quantification of mRNA using real-time RT-PCR, Nat Protoc, 1 (2006) 1559-82.

Norton, V.G., Imai, B.S., Yau, P. and Bradbury, E.M., Histone acetylation reduces nucleosome core particle linking number change, Cell, 57 (1989) 449-57.

Obara, I., Parkitna, J.R., Korostynski, M., Makuch, W., Kaminska, D., Przewlocka, B. and Przewlocki, R., Local peripheral opioid effects and expression of opioid genes in the spinal cord and dorsal root ganglia in neuropathic and inflammatory pain, Pain, 141 (2009) 283-91.

Ossipov, M.H., Kovelowski, C.J., Vanderah, T. and Porreca, F., Naltrindole, an opioid delta antagonist, blocks the enhancement of morphine-antinociception induced by a CCKB antagonist in the rat, Neurosci Lett, 181 (1994) 9-12.

Pan, Z.Z., mu-Opposing actions of the kappa-opioid receptor, Trends Pharmacol Sci, 19 (1998) 94-8.

Pan, Z.Z., Tershner, S.A. and Fields, H.L., Cellular mechanism for anti-analgesic action of agonists of the kappa-opioid receptor, Nature, 389 (1997) 382-5.

Pedersen, L.M., Jacobsen, L.M., Mollerup, S. and Gjerstad, J., Spinal cord long-term potentiation (LTP) is associated with increased dorsal horn gene expression of IL-1beta, GDNF and iNOS, Eur J Pain, 14 (2010) 255-60.

Pert, C.B. and Snyder, S.H., Opiate receptor: demonstration in nervous tissue, Science, 179 (1973) 1011-4.

Peterson, C.L. and Laniel, M.A., Histones and histone modifications, Curr Biol, 14 (2004) R546-51.

Qi, J. and Leahy, R.M., Resolution and noise properties of MAP reconstruction for fully 3-D PET, IEEE Trans Med Imaging, 19 (2000) 493-506.

Qi, J., Leahy, R.M., Hsu, C., Farquhar, T.H. and Cherry, S.R., Fully 3D Bayesian image reconstruction for the ECAT EXACT HR+, Nuclear Science, IEEE Transactions on, 45 (1998) 1096-1103.

Quock, R.M. and Vaughn, L.K., Do inhalation general anesthetic drugs induce the neuronal release of endogenous opioid peptides?, Life Sci, 77 (2005) 2603-10.

Radonic, A., Thulke, S., Mackay, I.M., Landt, O., Siegert, W. and Nitsche, A., Guideline to reference gene selection for quantitative real-time PCR, Biochem Biophys Res Commun, 313 (2004) 856-62.

Rady, J.J., Holmes, B.B. and Fujimoto, J.M., Antianalgesic action of dynorphin A mediated by spinal cholecystokinin, Proc Soc Exp Biol Med, 220 (1999) 178-83.

Randic, M., Jiang, M.C. and Cerne, R., Long-term potentiation and long-term depression of primary afferent neurotransmission in the rat spinal cord, J Neurosci, 13 (1993) 5228-41.

Rogan, M.T., Staubli, U.V. and LeDoux, J.E., Fear conditioning induces associative long-term potentiation in the amygdala, Nature, 390 (1997) 604-7.

Rosen, L.B., Ginty, D.D., Weber, M.J. and Greenberg, M.E., Membrane depolarization and calcium influx stimulate MEK and MAP kinase via activation of Ras, Neuron, 12 (1994) 1207-21.

Rygh, L.J., Svendsen, F., Hole, K. and Tjolsen, A., Natural noxious stimulation can induce long-term increase of spinal nociceptive responses, Pain, 82 (1999) 305-10.

Sandkuhler, J., Models and mechanisms of hyperalgesia and allodynia, Physiol Rev, 89 (2009) 707-58.

Schneider, F., Habel, U., Holthusen, H., Kessler, C., Posse, S., Muller-Gartner, H.W. and Arndt, J.O., Subjective ratings of pain correlate with subcortical-limbic blood flow: an fMRI study, Neuropsychobiology, 43 (2001) 175-85.

Schoultz, B., Marton, J., Hjørnevik, T., Reed, B., Willoch, F. and Henriksen, G., Synthesis and Evaluation of Three Structurally Related 18F-labeled Orvinols of Different Intrinsic Activities: [18F]FPEO, [18F]FBPN and [18F]FDPN, Manuscript in preparation (2012).

Schroeder, A., Mueller, O., Stocker, S., Salowsky, R., Leiber, M., Gassmann, M., Lightfoot, S., Menzel, W., Granzow, M. and Ragg, T., The RIN: an RNA integrity number for assigning integrity values to RNA measurements, BMC Mol Biol, 7 (2006) 3.

Schwarz, A.J., Danckaert, A., Reese, T., Gozzi, A., Paxinos, G., Watson, C., Merlo-Pich, E.V. and Bifone, A., A stereotaxic MRI template set for the rat brain with tissue class distribution maps and co-registered anatomical atlas: application to pharmacological MRI, Neuroimage, 32 (2006) 538-50.

Schweinhardt, P., Fransson, P., Olson, L., Spenger, C. and Andersson, J.L., A template for spatial normalisation of MR images of the rat brain, J Neurosci Methods, 129 (2003) 105-13.

Sgambato, V., Pages, C., Rogard, M., Besson, M.J. and Caboche, J., Extracellular signal-regulated kinase (ERK) controls immediate early gene induction on corticostriatal stimulation, J Neurosci, 18 (1998) 8814-25.

Sharpe, E.F., Kingston, A.E., Lodge, D., Monn, J.A. and Headley, P.M., Systemic pre-treatment with a group II mGlu agonist, LY379268, reduces hyperalgesia in vivo, Br J Pharmacol, 135 (2002) 1255-62.

Shih, Y.Y., Chen, Y.Y., Chen, C.C., Chen, J.C., Chang, C. and Jaw, F.S., Whole-brain functional magnetic resonance imaging mapping of acute nociceptive responses induced by formalin in rats using atlas registration-based event-related analysis, J Neurosci Res, 86 (2008) 1801-11.

Simmons, R.M., Webster, A.A., Kalra, A.B. and Iyengar, S., Group II mGluR receptor agonists are effective in persistent and neuropathic pain models in rats, Pharmacol Biochem Behav, 73 (2002) 419-27.

Spange, S., Wagner, T., Heinzel, T. and Kramer, O.H., Acetylation of non-histone proteins modulates cellular signalling at multiple levels, Int J Biochem Cell Biol, 41 (2009) 185-98.

Sugiura, Y., Lee, C.L. and Perl, E.R., Central projections of identified, unmyelinated (C) afferent fibers innervating mammalian skin, Science, 234 (1986) 358-61.

Svoboda, K.R. and Lupica, C.R., Opioid inhibition of hippocampal interneurons via modulation of potassium and hyperpolarization-activated cation (Ih) currents, J Neurosci, 18 (1998) 7084-98.

Tanic, N., Perovic, M., Mladenovic, A., Ruzdijic, S. and Kanazir, S., Effects of aging, dietary restriction and glucocorticoid treatment on housekeeping gene expression in rat cortex and hippocampus-evaluation by real time RT-PCR, J Mol Neurosci, 32 (2007) 38-46.

Taylor, S., Wakem, M., Dijkman, G., Alsarraj, M. and Nguyen, M., A practical approach to RT-qPCR-Publishing data that conform to the MIQE guidelines, Methods, 50 (2010) S1-5.

Terenius, L., Stereospecific interaction between narcotic analgesics and a synaptic plasm a membrane fraction of rat cerebral cortex, Acta Pharmacol Toxicol (Copenh), 32 (1973) 317-20.

Todd, A.J., Anatomy of primary afferents and projection neurones in the rat spinal dorsal horn with particular emphasis on substance P and the neurokinin 1 receptor, Exp Physiol, 87 (2002) 245-9.

Vanhoutte, P., Barnier, J.V., Guibert, B., Pages, C., Besson, M.J., Hipskind, R.A. and Caboche, J., Glutamate induces phosphorylation of Elk-1 and CREB, along with c-fos activation, via an extracellular signal-regulated kinase-dependent pathway in brain slices, Mol Cell Biol, 19 (1999) 136-46.

Vettese-Dadey, M., Grant, P.A., Hebbes, T.R., Crane- Robinson, C., Allis, C.D. and Workman, J.L., Acetylation of histone H4 plays a primary role in enhancing transcription factor binding to nucleosomal DNA in vitro, Embo J, 15 (1996) 2508-18.

Wang, X.J., Fan, S.G., Ren, M.F. and Han, J.S., Cholecystokinin-8 suppressed 3H-etorphine binding to rat brain opiate receptors, Life Sci, 45 (1989) 117-23.

Wang, X.J. and Han, J.S., Modification by cholecystokinin octapeptide of the binding of mu-, delta-, and kappa-opioid receptors, J Neurochem, 55 (1990) 1379-82.

Watkins, L.R., Kinscheck, I.B., Kaufman, E.F., Miller, J., Frenk, H. and Mayer, D.J., Cholecystokinin antagonists selectively potentiate analgesia induced by endogenous opiates, Brain Res, 327 (1985) 181-90.

Wiberg, M., Westman, J. and Blomqvist, A., Somatosensory projection to the mesencephalon: an anatomical study in the monkey, J Comp Neurol, 264 (1987) 92-117.

Wiesenfeld-Hallin, Z., Xu, X.J. and Hokfelt, T., The role of spinal cholecystokinin in chronic pain states, Pharmacol Toxicol, 91 (2002) 398-403.

Williams, J.T., Christie, M.J. and Manzoni, O., Cellular and synaptic adaptations mediating opioid dependence, Physiol Rev, 81 (2001) 299-343.

Willis, W.D., Long-term potentiation in spinothalamic neurons, Brain Res Brain Res Rev, 40 (2002) 202-14.

Willis, W.D. and Westlund, K.N., Neuroanatomy of the pain system and of the pathways that modulate pain, J Clin Neurophysiol, 14 (1997) 2-31.

Wimpey, T.L. and Chavkin, C., Opioids activate both an inward rectifier and a novel voltage-gated potassium conductance in the hippocampal formation, Neuron, 6 (1991) 281-9.

Woolf, C.J. and Salter, M.W., Neuronal plasticity: increasing the gain in pain, Science, 288 (2000) 1765-9.

Yang, D. and Gereau, R.W.t., Peripheral group II metabotropic glutamate receptors (mGluR2/3) regulate prostaglandin E2-mediated sensitization of capsaicin responses and thermal nociception, J Neurosci, 22 (2002) 6388-93.

Yang, H.W., Hu, X.D., Zhang, H.M., Xin, W.J., Li, M.T., Zhang, T., Zhou, L.J. and Liu, X.G., Roles of CaMKII, PKA, and PKC in the induction and maintenance of LTP of C-fiber-evoked field potentials in rat spinal dorsal horn, J Neurophysiol, 91 (2004) 1122-33.

Zhang, X., Dagerlind, A., Elde, R.P., Castel, M.N., Broberger, C., Wiesenfeld-Hallin, Z. and Hokfelt, T., Marked increase in cholecystokinin B receptor messenger RNA levels in rat dorsal root ganglia after peripheral axotomy, Neuroscience, 57 (1993) 227-33.

Zhang, Z., Cai, Y.Q., Zou, F., Bie, B. and Pan, Z.Z., Epigenetic suppression of GAD65 expression mediates persistent pain, Nat Med, 17 (2011) 1448-55.

Zhao, X.Y., Liu, M.G., Yuan, D.L., Wang, Y., He, Y., Wang, D.D., Chen, X.F., Zhang, F.K., Li, H., He, X.S. and Chen, J., Nociception-induced spatial and temporal plasticity of synaptic connection and function in the hippocampal formation of rats: a multi-electrode array recording, Mol Pain, 5 (2009) 55.

Zubieta, J.K., Smith, Y.R., Bueller, J.A., Xu, Y., Kilbourn, M.R., Jewett, D.M., Meyer, C.R., Koeppe, R.A. and Stohler, C.S., Regional mu opioid receptor regulation of sensory and affective dimensions of pain, Science, 293 (2001) 311-5.

Appendices

Appendix I: RNA isolation

Procedure for RNA isolation:

1. Hippocampal tissue was transferred to a pre-cooled 2.0 ml PCR clean eppendorf tube and 0.8 ml TRIzol was added.
2. Three sterile metal balls were added to each sample, and the tissue was homogenized by aid of a mixer mill. Frequency 30, time 4 x 30 sec.
3. The sample was incubated at room temperature (RT) for 5 min.
4. The sample was centrifuged at 12 000 g for 5 min at 4 °C. The supernatant was transferred to a new eppendorf tube.
5. 0.2 ml chloroform was added. The sample was shaken vigorously by hand for 15 sec, and incubated for 3 min at RT.
6. The sample was centrifuged at 12 000 g for 15 min at 4 °C.
7. The water phase was transferred to a new eppendorf tube, 10-200 µl at each time. 0.5 ml isopropanol was added. The contents were mixed well and incubated at RT for 10 min.
8. The sample was centrifuged at 12 000 g for 15 min at 4 °C.
9. The supernatant was removed (800 µl at first, then 200 µl), and the RNA pellet was washed with 1ml 75% EtOH (in DEPC water), mixed, and vortexed.
10. The sample was centrifuged at 12 000 g for 5 min at 4 °C.
11. The supernatant was removed. The pellet was dried for 15-20 min at RT, dissolved in 12 µl DEPC-water, and kept on ice.
12. The sample was incubated at 65 °C for 10 min, placed on ice, spun, placed back on ice, and mixed by a pipette.
13. A 100 x dilution was made to establish RNA concentration: 1 µl sample + 100 µl TE-buffer were mixed and vortexed. The RNA concentration was estimated from the optical density of the solution at 230 nm, 260 nm, and 280 nm. Slit = 0.5 nm.
14. The sample was diluted to 0.5 µg/µl by adding x.x µl DEPC-water: ((10 µl x concentration µg/µl) / 0.5 µg/µl)) – 10 µl = x.x µl DEPC-water to add.
15. The sample was stored at – 80 °C.

DEPC-water:

1. DEPC was added to H_2O to a final concentration of 0.1% in a capped bottle and mixed well.
2. The DEPC/ H_2O bottle was shaken vigorously and placed under a fume hood over night without the bottle cap.
3. The DEPC/ H_2O bottle was autoclaved for 20 min and placed in the refrigerator.

TE-buffer:

DEPC/ H_2O were added 0.5 M EDTA (pH 8) to a final concentration of 0.1 mM and 1 M Tris-HCl (pH 8) to a final concentration of 10 mM.

Appendix II: Evaluation of RNA quality

Procedure for evaluation of RNA quality by on-chip electrophoresis (Agilent 2100 Bioanalyzer):

The reagents were allowed to equilibrate to room temperature for 30 min before use.

1. 550 µl of the RNA 6000 Nano gel matrix was transferred to a spin filter, and centrifuged at 1500 g for 10 min. 65 µl of the filtered gel was transferred to a 0.5 ml microfuge tube.
2. The RNA 6000 Nano dye concentrate was vortexed for 10 sec and spun down. 1 µl of the dye was added to the filtered gel. The solution was vortexed well, and centrifuged at 13 000 g for 10 min.
3. The RNA samples were diluted to a final concentration of 300 ng/µl, and heat denatured at 70 °C for 2 min.
4. 350 µl of RNase Zap was loaded to a microchip, and run for 1 min on the Bioanalyzer for decontamination of the electrodes. The procedure was repeated with 350 µl RNase-free water for 10 sec.
5. 9 µl of the gel-dye mix was loaded to the well marked ^G on a new RNA 6000 Nano microchip.
6. The microchip was mounted on the chip priming station. The priming station was closed and pressure was applied to the microchip for 30 sec by a plunger.
7. 9 µl of the gel-dye mix were loaded to the wells marked G.
8. 5 µl of the RNA 6000 Nano marker were loaded to all 12 test-wells and to the ladder-well.
9. The standard ladder was heat denatured at 70 °C for 2 min. 1 µl of the ladder was loaded to the well marked with the ladder.
10. 1 µl of the samples were loaded to the test-wells.
11. The microchip was vortexed at 2400 rpm for 1 min, and run on the Bioanalyzer.
12. After the Bioanalyzer had completed the analysis-program, 350 µl of RNase-free water was loaded to a microchip and run for 10 sec on the Bioanalyzer for decontamination of the electrodes.

Appendix III: cDNA synthesis

Procedure for cDNA synthesis:

All reagents were from “First Strand cDNA Synthesis Kit for RT-PCR (AMV)” (Roche Diagnostics, Mannheim, Germany).

All reagents and samples were kept on ice when not otherwise specified.

1. 3.0 µl of RNA was mixed with water to a total volume of 4.5 µl in 0.5 ml eppendorf tubes.
2. Mixture 1 was prepared:

Reagent	volume/sample
Random primer p(dN)6	1.50 µl
Deoxynucleotide-mix	1.50 µl
Total	3.0 µl

3. 3 µl of mixture 1 was added to each sample. Tubes were vortexed and spun down.
4. The tubes were incubated at 65 °C for 15 min.
5. Mixture 2 was prepared:

Reagent	volume/sample
10 x reaction buffer	1.50 µl
25 mM $MgCl_2$	3.00 µl
RNase inhibitor 50 u/ µl	0.68 µl
AMW reverse transcriptase	0.50 µl
dH_2O	1.80 µl
Total	7.51 µl

6. The PCR machine was heated to 42 °C.
7. 7.5 µl of mixture 2 was added to each tube. The tubes were briefly vortexed and spun down.
8. The reverse transcription reaction was run on the PCR machine at the following program: 42 °C 60 min, 99 °C 5 min, and 4 °C 5 min.
9. Each sample was added 135 µl of TE-buffer, mixed and spun down.
10. The samples were stored at – 80 °C.

Appedix IV: Quantitative polymerase chain reaction (qPCR)

Procedure for qPCR analysis of Oprm1/Oprk1/PENK/CCK_B gene expression:

All reagents and samples were kept on ice when not otherwise specified.

1. A master mix was prepared:

Reagent	volume/sample
ddH_2O	5.0
Power SYBR green master mix	9.6 µl
Primer forward (25 pmol/µl)	0.20 µl
Primer reverse (25 pmol/µl)	0.20 µl
Total	15 µl

2. The cDNA samples used for β-actin analysis were diluted: 1 µl cDNA (10 ng/µl) + 9 µl ddH2O.
3. 8 µl from three different cDNA samples (10 ng/µl) were mixed to give a stock cDNA solution. A dilution series used to generate a standard curve for each gene was prepared:

Dilution series nr.	cDNA	ddH_2O
1	4.35 µl	Undiluted
2	6 µl	+ 18 µl
3	6 µl from nr 2	+ 18 µl
4	6 µl from nr 3	+ 18 µl
5	6 µl from nr 4	+ 18 µl
6	6 µl from nr 5	+ 18 µl

4. 15.65 µl master mix was loaded to each well on a 96 well plate.
5. 4.35 µl ddH_2O were added to the non-template control wells.
6. 4.35 µl sample cDNA, or pre-diluted samples for β-actin analysis, or dilution series samples were transferred to the PCR-plate in two parallels, and mixed well.
7. The PCR plate was sealed with a plastic film and spun down. A rubber mat was placed on top of the PCR plate.
8. The qPCR reaction was run at the following schedule: 95 °C 2 min, followed by 40 cycles of 95 °C 10 sec, and 60 °C 30 sec.